Contents — G through O

EXPERIMENTAL MODELING OF IMPACT-INDUCED HIGH-TEMPERATURE PROCESSING OF SILICATES. M.V.Gerasimov[1], Yu.P.Dikov[2], and O.I.Yakovlev[3]. [1]Space Research Institute, RAS, Moscow 117997, Profsoyuznaya st., 84/32, mgerasim@mx.iki.rssi.ru, [2]Institute of Ore Deposits, Petrography, Mineralogy and Geochemistry, RAS, Moscow 109017, Staromonetny per., 35, dikov@igem.ru, [3]Vernadsky Institute of Geochemistry and Analytical Chemistry, RAS, Moscow 117975, GSP-1, Kosygin st., 19, yakovlev@geokhi.ru.

Introduction: Large scale impacts of asteroids and meteorites play an important role in the evolution of planets and their satellites. Pulse input of huge energy during an impact results in noticeable changes in both mechanical and geochemical state of colliding material. The complexity of geochemical processes during an impact suggests experimental modeling as the main tool of its investigation rather than computing approach. On the other side, the modeling of mechanical issues of large scale impacts is mainly a success of computations. We need to have a good cooperation between both computer modeling of mechanical issues of an impact and experimental investigations of geochemical processes to build up a more or less realistic picture of a large-scale impact.

Experimental investigation of high-temperature modification of silicates. Experiments were done by use of hypervelocity gun facilities and laser pulse installation [1]. Some principal effects of high-temperature processing of silicates are:

Formation of clusters during vaporization. Volatilization of elements during impact-induced vaporization proceeds not only as classical volatilization of atoms and oxides but by formation of molecular clusters which can assemble a number of elements with different individual volatility. Experiments prove the formation of "enstatite", "netheline", and "wollastonite" clusters [2,3]. The formation of clusters provides less specific energy of vaporization of silicates compared to that calculated in assumption of total dissociation of materials and must be accounted for in computations.

Noticeable redox processes. The main element of silicates is oxygen which is also mobile during high-temperature processes and provide noticeable redox processes in the system. Experiments indicate simultaneous formation of mainly all possible redox states of elements [4]. Highly oxidized states of elements coexist with their reduced states. Phases of reduced carbon, iron, and other elements can be formed during impacts despite of oxidizing conditions.

Abnormal volatility of refractory elements. Experiments show a rather high mobility of elements which are usually considered as refractory and are accounted for as indicators of parts of different materials during mixing [5]. Among such elements are REE, highly siderophile elements (HSE), and other. The mechanism of abnormal volatility need more investigation but it can be a result of formation of specific clusters. HSE can be mobilized into forming and dispersing metallic iron droplets [6].

Problem of mixing of colliding materials. Chemical composition of forming objects during an impact is the result of mixing of parts from naturally heterogeneous projectile and target materials and also due to selective mobility of elements. The mixing of projectile and target materials does not have sufficient coverage by computing modeling and the estimation of the volume and degree of mixing is still uncertain. Usually, the input of projectile material is considered by an account for of the increase of HSE in impactites and by isotopical considerations. None of methods is strict and can be applied only to individual samples. There is a reasonable deficit of impactites which represents a pure projectile material. Mixing seems to be a valuable factor of modification of projectile material and it should be considered using computing methods. The mechanism of mixing of projectile and target materials probably can be simulated involving Kelvin-Helmholtz and/or Reyley-Taylor instability mechanisms.

Experimental investigation of the possibility of impact-induced formation of so called "pristine" lunar glasses shows that they could be formed by an impact of a chondritic projectile into lunar basalts. The mixing of basaltic and chondritic materials together with high-temperature processing develop impact glasses with the composition similar to lunar "pristine" glasses, which is characterized by: high Mg/Mg+Fe ratio, high Al/Mg ratio, homogeneity, surface correlated volatiles, etc. [7]. The formation of metallic iron drops and their dispersion from high-temperature melts is an important mechanism for depletion of silicate melts in siderophile elements and for formation of agglutinitic glasses.

Acknowledgment. The research was supported by RFBR grant No 01-05-64564.

References: [1] Gerasimov M.V. et al. (1998) *Earth, Moon, and Planets*, *80*, 209-259. [2] Dikov Yu.P., et al. (1994) *LPSCXXV,* 329-330. [3] Yakovlev O.I., et al. (1996) *Geochem. Intern.*, *34*, No. 8, 706-713. [4] Yakovlev O.I., et al. (1993) *Geochem. Intern.*, *30*, No. 7, 1-10. [5] Dikov Yu.P., et al. (1992) *Geokhimiya*, № 2, 291-296 (Rus.). [6] Yakovlev O.I., et al. (2002) *LPSCXXXIII,* #1271 (CD-ROM). [7] Yu.P. Dikov et al. (2001) *LPSCXXXII,* #1559 (CD-ROM).

THERMAL AND DYNAMIC CONSEQUENCES OF IMPACT – LESSONS FROM LARGE IMPACT STRUCTURES. Roger L. Gibson and W. Uwe Reimold, Impact Cratering Research Group, School of Geosciences, University of the Witwatersrand, Private Bag 3, P.O. Wits 2050, Johannesburg, South Africa (E-mail: 065rlg@cosmos.wits.ac.za, reimoldw@geosciences.wits.ac.za).

Introduction: In the early years following the recognition of meteorite impact cratering as an important geological process within the Solar System, impact researchers were largely confined to inferring cratering mechanics from studies of surface crater morphologies and small-scale experiments. With the advent of sophisticated computer-based numerical simulations and high-resolution geophysics, however, researchers have begun to explore more fully the detailed 3-D structure of craters and the processes that give rise to them. This paper examines some of the issues raised by the model simulations from the perspective of the field evidence presented in impact structures, with particular reference to the Vredefort structure in South Africa.

Reality vs simulation: Impact is a short-term catastrophic process driven by the transfer of the kinetic energy of a hypervelocity projectile into a target. At a first-order approximation, the cratering process varies as a function of energy released by the impact – small impacts create simple craters whereas larger events create complex craters with central uplifts, peak rings or multiple rings. Projectiles of varying sizes, densities and velocities can effectively release similar amounts of energy and, thus, create similar structures. Additional levels of complexity can be added by varying, inter alia, the shape of the impactor, the angle of impact, and the structure and composition of the target. To a large extent, numerical simulations have allowed researchers to experiment with a wide range of input parameters and to examine the consequences of changing these variables (e.g. [1], [2]). The question remaining, however, is whether direct observation of impact structures in the field and laboratory-based experimental work can facilitate further refinement of such simulations.

The Vredefort impact structure: The 2.02 Ga Vredefort impact structure in South Africa is the world's oldest impact structure. It may lay claim to being the largest as well, however, substantial erosion (by between 7 and 10 km) has obliterated the original crater rim and impact breccias. Like the similarly large 1.85 Ga Sudbury structure, Vredefort has attracted the attention of numerical modelers (e.g. [3], [4]) in part because the high levels of erosion require indirect estimation of the size of the respective impact events and craters. In the Vredefort structure, the root zone of the central uplift – the ~90-km-wide Vredefort dome – is the best-preserved part, although impact-related structural and hydrothermal effects are evident up to radial distances of at least 100 km from the center, and possibly further afield as well. Shock effects (shatter cones, planar deformation features, high pressure quartz polymorphs and textures suggestive of diaplectic glass and mineral melt formation) are confined to the dome, and display a distribution consistent with a broad increase in maximum shock pressure radially inwards ([5], [6]). A similar broad increase in the grade of shock-induced thermal metamorphism is observed towards the center of the dome ([6]-[8]). In addition, dykes of impact melt and voluminous pseudotachylitic breccias are present in the rocks. Therriault et al. [9] estimated an original crater diameter of 270 to 300 km based on the distribution of the shock features. Henkel and Reimold [10] obtained a similar estimate from geophysical modeling. Numerical simulations by Turtle and Pierazzo [4, 11], however, have suggested a diameter as small as 120-160 km. These scaling simulations used the distribution of common shock effects such as PDFs in quartz, and the distribution of post-shock isotherms, respectively, as a basis for reconstructing the impact crater. Clearly, such a wide discrepancy requires further scrutiny. A critique of the modeling parameters and assumptions is beyond the scope of this paper. Instead, we wish to focus on the geological evidence within impact structures such as Vredefort that can assist in understanding the cratering process.

The problem with impact structures: The fundamental problem with impact structures is that their large-scale order and symmetry disguises the chaotic nature of their constituent features at smaller scales. The heterogeneous nature of shock wave interaction with rocks at the grain scale has long been known from experimental and field studies, yet the principal aim of integrating observational data from partially eroded structures such as Vredefort and Sudbury with simulation results is to obtain a match between the large-scale morphology and the spatial distribution of peak shock isobars and post-shock isotherms, on the one side, and the model results on the other. Model predictions for complex impact structures (e.g., [3], [12]) are that the shock effects are largely confined to the central uplift and that the radial inward movements that accompany central uplift formation modify the original hemispherical pattern of shock isobars into an elongate bulbous shape with a vertical long axis. As post-shock temperatures are directly proportional to the magnitude of the shock, they will display a similar elongate bulbous pattern, enhanced by interaction between the shock heating and the heat already present in the rocks

due to the pre-impact geotherm [3]. At the large scale, results from the Vredefort dome have confirmed the simulation predictions. In fact, Melosh and Ivanov's [12] and Ivanov and Deutsch's [3] results were instrumental in directing geological investigations to the central parts of the dome where the models predicted shock pressures as high as 60 GPa and post-shock temperatures in excess of 1000 °C. Whereas a previous study based on quartz PDFs in the dome by Grieve et al. [13] had been unable to confirm shock pressures of more than 10-15 GPa in these rocks, but had speculated that pressures may have been as high as 25 GPa, these studies confirmed widespread shock metamorphism of feldspars and hydrous ferromagnesian silicates at pressures in excess of 30 GPa and possibly as high as 50 GPa ([5], [6]), and post-shock temperatures of between 1000 and 1350 °C ([6], [8]). These results confirmed Grieve et al.'s [13] original contention that post-shock annealing in the core of the dome had selectively annealed PDFs, rendering the pressure estimation technique useless.

Whilst the modeling predictions and direct observations concur on the broad scale, it is important to note that Ivanov and Deutsch's [3] models are for a 200-250 km diameter structure whereas [4, 11] maintain that they have achieved good agreement with a 120-160 km diameter structure. Apart from the heterogeneous grain-scale response to shock noted from experimental studies and many other impact structures, our group has recently established larger-scale heterogeneity in the formation of pseudotachylite veins in the dome that suggests that shock pressures varied by as much as a factor of 2-3 on scales ranging from millimeters to tens of meters. This finding, which is attributed to complex reflection and refraction of the impact shock wave through the target rocks as a result of preexisting heterogeneities, not only makes the immediate geological context in which samples for "average" peak pressure calculations are chosen of extreme importance, but also questions whether such an "average" pressure approach is realistic. The link between peak shock pressure and post-shock temperature means that this also has implications for "average" post-shock isotherms. Gibson [8] has noted highly variable post-shock metamorphic textures in rocks in the dome and widespread evidence of disequilibrium that confirm localized thermal heterogeneity. A similar conclusion was drawn by [14] from the deep borehole through the Puchezh-Katunki central uplift.

A further issue with estimation of peak shock pressures in impact structures relates to the reliability of shock experimental data in constraining peak shock pressures in natural events. [15] have recently reviewed the problems in extrapolating data from experiments to natural rocks. They caution that, because of the short duration of experiments relative to natural events, and even the design of some of these experiments, threshold pressures for the formation of certain shock effects may be considerable overestimates. Such a breakdown in basic knowledge would have fundamental implications when attempting to use shock isobar patterns to refine numerical simulations.

In addition to the shock and thermal patterns generated by an impact cratering event, numerical simulations are attempting to explain how, on a gross scale, a well-ordered structure evolves. The Vredefort dome provides a rare opportunity to access large areas of rock from deep levels within the central uplift and to test whether models such as acoustic fluidization [12] or the block model [3] can explain central uplift formation. Preliminary data from the dome by our group have failed to identify pervasive block rotation, even where substantial pseudotachylitic melts are likely to have existed during central uplift formation. Most movements appear to reflect late-stage extensional collapse of the structure along faults at a variety of scales. Further from the central uplift, impact-related deformation involves brittle-ductile folding and extensional faulting on scales of tens of meters to kilometers that also appears to be related to the latter stages of central uplift formation.

Summary: At present, numerical modeling of large impact events provides a good first-order indication of the distribution of impact-related features. However, the low spatial resolution of the models (typically of the order of kilometers) hampers full integration of the modeling results with the observed geological features and does not allow the latter to be used to refine model parameters. More work is needed to understand the local-scale interaction between a shock wave and its target rocks to assist resolution of this problem.

References: [1] Pierazzo E. and Melosh H.J. (1999) *EPSL, 165,* 163-176. [2] Ivanov B.A. and Artemieva N.A. (2002) *GSA Spec. Pap., 356,* 619-630. [3] Ivanov B.A. and Deutsch A. (1999) *GSA Spec. Pap., 339,* 389-397. [4] Turtle E.P. and Pierazzo E. (1998) *MAPS, 33,*483-490. [5] Gibson R.L. et al. (2001) *LPS XXXII,* Abstract #1012. [6] Gibson R.L. et al. (2002) *Geology, 30,* 475-478. [7] Gibson R.L. et al. (1998) *Geology, 26,* 787-790. [8] Gibson R.L. (2002) *JMG, 20,* 57-70. [9] Therriault A.M. et al. (1997) *MAPS, 32,* 71-77. [10] Henkel H. and Reimold W.U. (1998) *Tectonophys., 287,* 1-20. [11] Turtle E.P. and Pierazzo E. *Geology*, submitted. [12] Melosh H.J. and Ivanov B.A. (1999) *Ann. Rev. EPS, 27,*385-415. [13] Grieve R.F. et al. (1990) *Tectonophys., 171,* 185-200. [14] Masaitis V. (1999) *MAPS, 34,* 691-711. [15] DeCarli P.S. et al. (2002) *GSA Spec. Pap. 356,* 595-605.

TWO- AND THREE-DIMENSIONAL SIMULATIONS OF ASTEROID OCEAN IMPACTS. G. Gisler, R. P. Weaver, C. L. Mader[1] and M. L. Gittings[2], [1]Los Alamos National Laboratory, MS T087, Los Alamos NM 87545 USA, [2]Science Applications International MS T087, Los Alamos NM 87545 USA

We have performed a series of two-dimensional and three-dimensional simulations of asteroid impacts into an ocean using the SAGE code from Los Alamos National Laboratory and Science Applications International Corporation. The SAGE code is a compressible Eulerian hydrodynamics code using continuous adaptive mesh refinement for following discontinuities with a fine grid while treating the bulk of the simulation more coarsely. We have used tabular equations of state for the atmosphere, water, the oceanic crust, and the mantle. In two dimensions, we simulated asteroid impactors moving at 20 km/s vertically through an exponential atmosphere into a 5 km deep ocean. The impactors were composed of mantle material (3.32 g/cc) or iron (7.8 g/cc) with diameters from 250m to 10 km. In our three-dimensional runs we simulated asteroids of 1 km diameter composed of iron moving at 20 km/s at angles of 45 and 60 degrees from the vertical. All impacts, including the oblique ones, produce large underwater cavities with nearly vertical walls followed by a collapse starting from the bottom and subsequent vertical jetting. The initial asymmetry of the oblique-impact transient crater does not persist beyond the first two minutes. Substantial amounts of water are vaporized and lofted high into the atmosphere. In the larger impacts, significant amounts of crustal material are lofted as well. Tsunamis up to a kilometer in initial height are generated by the collapse of the vertical jet. These waves are initially complex in form, and interact strongly with shocks propagating through the water and the crust. The tsunami waves are followed out to 100 km from the point of impact. Their periods and wavelengths show them to be intermediate type waves, and not (in general) shallow-water waves. At great distances, the waves decay faster than the inverse of the distance from the impact point, ignoring sea-floor topography.

A point of crucial interest is to determine the smallest asteroid for which widespread tsunami damage might be expected. To address this, we paid special attention to the wave heights generated by the vertical impacts we simulated, and the attenuation of these heights as a function of distance away from the impact point. We placed massless tracer particles on the water surface at the initial time and tracked their positions throughout the simulations. For the smaller impactors, the tracer particles executed roughly elliptical trajectories that almost (but didn't quite) close upon themselves. For the more massive impactors, the tracer trajectories were extremely complex and difficult to resolve into simple waves. Because the tracers tended to drift away from the surface, it was insufficient to track the maximum heights reached by the tracers. Instead, we measured the amplitudes of the maximum excursions from mean tracer-particle position as a function of distance from the point of impact. These amplitudes are plotted in Figure 1, where it is seen that for all six cases in our parameter study, the waves decay with distance r from the impact point faster than $(1/r)$. The power-law indices for the least-squares fits plotted vary from –2.25 to –1.3.

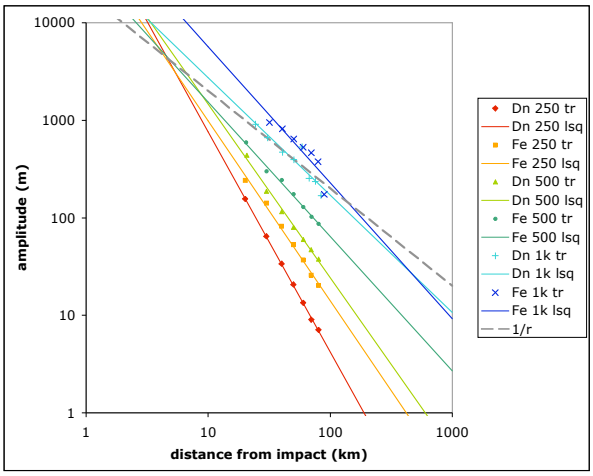

Figure 1. Tracer-particle amplitudes in asteroid-generated tsunami waves decline faster than the inverse of the distance from the impact point.

In all cases we investigated, the waves are extremely dissipative, compared to other types of tsunamis or other waves on water. The reason for this is that the perturbation giving rise to the waves, namely the impact of the asteroid and the immediate vaporization of the water along the path of entry, is hypersonic and a complex system of shocks is initiated in the water, the air, and the ocean floor basalt. The interaction of these shocks with each other and with the bounding surfaces (the air-water interface and the water-crust interface) keeps perturbing the waves that are generated so that the motion becomes, and remains, highly turbulent. This is illustrated in Figure 1, where we plot, in grayscale, density (top) and pressure (bottom) for a small portion of the computational domain near the leading wave, 34 kilometers distant from, and 5 minutes after, the impact event. Evident in the pressure plot is the highly turbulent, post-shock, atmosphere, which continues to extract energy from the propagating wave. Turbulence within the water gives rise to continued cavitation often (but not always) closely associated with the wave crests. In this frame we see the remnant of a collapsed cavitation bubble, together with the backward-propagating shock caused by its recent

collapse.

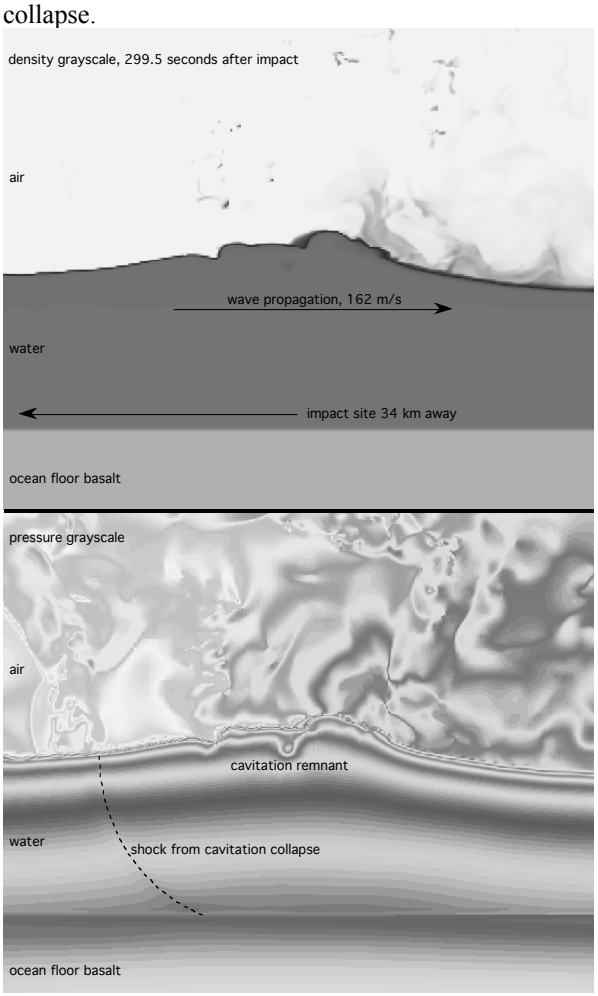

Figure 2. Plots of density (top) and pressure (bottom) in a small part of the computational volume near the crest of the leading wave in one of our simulations show evidence of continuing energy dissipation long after the impact event.

Both the extraction of wave energy by the atmosphere and the continuous generation of turbulence and cavitation within the water cause the waves to be highly dissipative; these waves are very far from energy-conserving. Unlike tsunamis generated by earthquakes or landslides, these waves decay rather more rapidly than the 1/r law expected for energy-conserving waves.

Moreover, the velocities and periods for these waves, plotted in Figure 3, are both rather less than those expected for the classical shallow-water waves generated by the usual sources of tsunamis. Both these considerations argue against significant ocean-wide damage associated with waves generated by small asteroids. To make this statement with more precision, let us establish a criterion for ocean-wide concern, in particular a one-meter wave amplitude at a distance of 1000 km from the impact event. With this criterion, the threshold of concern indicated by our simulations is the impact of a 1000m diameter dunite asteroid at 20 km/s. Anything smaller falls below the criterion postulated above for ocean-wide damage.

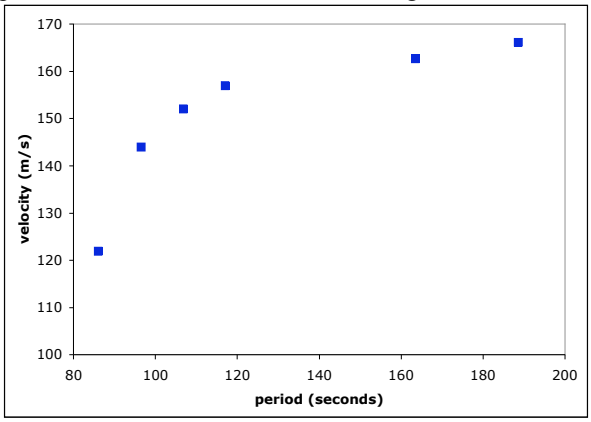

Figure 3. Velocities and periods for asteroid-induced waves are both smaller than the shallow-water values (221 km/s and ~600 seconds, in a 5-km deep ocean) expected and observed for earthquake and landslide induced tsunamis.

In fact it may even be arguable whether we are entitled to designate asteroid-impact generated waves as tsunamis, properly defined. Because of the highly dissipative and turbulent character of these waves, so different from classical tsunamis, we may need to refine our terms.

The potential for significant damage from ocean impacts of smaller asteroids must not be understated, however. The criterion adopted above (1m amplitude at 1000 km) ignores the geographical fact there are few if any parts of the earth's ocean less than 1000 km from land. Thus, while ocean-wide damage would not be expected from a 100m asteroid, for example, significant local damage will likely occur. Even for such a relatively small projectile, the input of energy to the atmosphere may be significant enough to cause disastrous (though local) firestorms.

We have also ignored ocean-floor topography in this study, and it is known that (at least for classical tsunamis) amplitudes increase dramatically as the water depth diminishes near shore. We have just begun some studies to determine if this phenomenon generalizes to impact-generated waves as well.

We acknowledge useful discussions with Erik Asphaug, Rob Coker, Jack Hills, Jay Melosh, and Steven Ward. Bob Boland and Lori Pritchett helped us run the simulations, and machine time was provided by the DOE's program in Advanced Simulation and Computing.

OBSERVATIONS OF THE TERRESTRIAL IMPACT CRATERING RECORD

R.A.F. Grieve, Earth Sciences Sector, NRCan, 588 Booth Street, Ottawa, ON K1A 0Y7, CANADA. (rgrieve@nrcan.gc.ca)

Introduction: The currently known terrestrial record of impact cratering stands at over 160 impact structures and several new examples are identified each year (1). The record, however, is a biased sample of an originally much larger population, favoring younger, larger structures in geologically stable areas of the Earth's continental crust. The largest and oldest known structures are limited to diameters of ~ 250-300 km and ages of < 2 Ga. Care must be taken, therefore, in making generalised statements regarding the record with respect to such time-integrated effects as variations in cratering rate, periodicities, etc. (e.g., 2). The terrestrial record, however, does provide cumulative observations of aspects of the cratering process and is the only available source of ground truth with respect to the structural and lithological results of large-scale natural impact events.

Some critical observations: Although attribution is often open to dispute, it is clear that detailed studies at a select number of terrestrial impact structures have provided important boundary constraints on aspects of cratering processes. Impact craters are three-dimensional structures and the ability to drill and recover core, to conduct multi-parameter geophysical surveys and to observe impact craters of similar size and morphology at different erosional levels is the ultimate strength of the terrestrial record. Concepts such as transient cavities formed by excavation and displacement and the collapse of transient cavity walls in simple craters have resulted (e.g., 3). Similarly, the confinement of significant excavation to only the central volume, with the structural preservation of near-surface lithologies exterior to this volume and the structural uplift of originally deeper-seated lithologies in the center of complex structures can be traced, in large part, to detailed and repeated observations of terrestrial impact craters (e.g., 4). Similarly, effects associated with shock metamorphism of various rock types and how its manifestation can differ (e.g., in porous targets) preceded and moved in parallel with shock-recovery experimentation. Observations have been particularly useful in understanding the effects of shock loading in the upper range of experimentally generated shock stresses, such as those leading to impact melting (e.g., 5).

Some less certain observations: Morphometric relations for terrestrial structures have been defined but are subject to considerable uncertainty, due to the effects of erosion and the statistics of small numbers (4). While it is only the more pristine terrestrial examples that can be used to define morphometries, the situation is exacerbated by the fact that many terrestrial impact craters have been studied in insufficient detail or without modern understanding of impact processes. In some cases, the literature is confined essentially to the "discovery" publication or dates from pre-Apollo to periods between Apollo missions, which were a major driver for the study of terrestrial impact structures. The impetus provided by the Apollo program has been replaced to some degree by economic and biosphere drivers. In the

U.S., government funding for studies at terrestrial impact structures appears to fall between the responsibilities of both NASA and NSF. This has tended to favor modelling studies at the expense of field work. It is clearly less costly to engage in modelling studies, but how can we, as a community, evaluate the veracity of the models without observational data from the field? (e.g., 6,7). Experimental data will not suffice to fill this gap, as there are problems with scale and understanding of the physical properties of the relevant materials, despite innovative procedures to compensate for them (e.g., 8). It is true, however, it is easier to connect observational data to later-time cratering processes because that is what they more closely reflect, representing as they do the end of the cratering process. Conversely, modeling has traditionally focussed on more early time processes in cratering events. Clearly, there are opportunities for closer partnerships of observational and modeling studies. The probem, however, is often that no one wants to be the bridesmaid!

Some closing thoughts on observations: We are very much prejudiced by the appearance of fresh lunar craters. It is the database with which we are most familiar regarding crater morphology. It is a fact, however, that some of the younger (fresher) complex craters on Earth (e.g., Ries, Haughton, Zhamanshin) do not have an emergent central peak, yet other, albeit buried, structures do (e.g., Boltysh, Moljnir). This begs a very fundamental question: Why? At first glance, it would appear to be a target effect, with the latter formed in crystalline targets and the former in mixed targets. There is also the question of the occurrence of ring or multi-ring basins on Earth (e.g., 9). Several structures have been "proposed" as ringed basins — Manicouagan, for instance. The question is, however, are these rings erosional artefacts? Among the larger structures is Chicxulub – again proposed as a ring structure — but it is buried and inferences rely upon (sometimes conflicting) interpretations of geophysical data (e.g., 10). Drilling at Chicxulub to date has served little to address this problem. Sudbury is also often portrayed as a terrestrial example of a multi-ring basin. There are rings of pseudotachylite, or so the limited pattern of exposed outcrops suggests (e.g., 11). If these do, in fact, exist, what is their relation to the megascarps in lunar basins? Model calculations, albeit simplistic, suggest that the high-gravity environment of Earth will not necessarily produce basins in the same size range as the large multi-ring basins of the moon, due to the increased relative proportion of impact melt to cavity volume on Earth.

References: (1) www.unb.ca/passc/ImpactDatabase. (2) R. Grieve (2001) In *Accretion of Extraterrestrial Material throughout Earth's History*, Kluwer, 379-399. (3) M. Dence *et al.* (1977) In *Impact and Explosion Cratering*, 247-276, Pergamon. (4) R. Grieve & M. Pilkington (1996) *Jour. Aust. Geol. Geophy.* **16**, 399-420. (5) J. Whitehead *et al.* (2002) *MAPS* **37**, 623-647. (6) A. Therriault *et al.* (1997) *MAPS* **32**, 71-77. (7) E. Turtle and E. Pierazzo (1998) *MAPS* **33**, 483-490. (8) K. Housen *et al.* (1999) *Nature* **402**, 155. (9) R. Grieve & A. Therriault (2000) *Ann. Rev. Earth Planet. Sci* **28**, 305-338. (10) J. Morgan *et al.* (2002) GSA Sp. Pap. 356, 39-46. (11) J. Spray & L. Thompson (1995) *Nature* **373**, 130-132.

LIMITS TO THE PRESENCE OF IMPACT-INDUCED HYDROTHERMAL ALTERATION IN SMALL IMPACT CRATERS ON THE EARTH: IMPLICATIONS FOR THE IMPORTANCE OF SMALL CRATERS ON MARS. H. E. Newsom and Hagerty J. J., University of New Mexico, Institute of Meteoritics, Dept. of Earth & Planetary Sciences, Albuquerque, NM 87131 U.S.A. Email: Newsom@unm.edu

Introduction: Impact craters on the earth contain evidence for hydrothermal activity. An important property of small craters is the limit to the amount of energy deposited during the impact that can lead to hydrothermal activity. Hydrothermal activity is potentially important for producing alteration minerals, trapping water, and transporting mobile elements to the martian surface. Hydrothermal systems in impact craters may also be important for astrobiological investigations in terms of providing environments for organic chemical processes to occur and as near-surface locations that could be easily investigated by surface exploration missions [1]. Another important reason for understanding the lower limit on thermal effects for small craters is in the use of small superimposed craters as probes of larger craters during surface missions. If hydrothermal material is found associated with superimposed craters it will be important to distinguish between hydrothermal events associated with the earlier versus the later crater. In the future, comparisons of our observations with numerical models for the formation of small craters can lead to a better understanding of the role of small craters on Mars.

Lonar Crater: The 50,000 year old, 1.8km diameter Lonar crater is located in Maharashtra, India (19º58'N, 76º31'E) [2]. This relatively small crater is of particular interest because of its unique morphological and mineralogical properties, which make it a valid analogue for similar craters on the surface of Mars [2, 3]. We show that even in this relatively small crater substantial hydrothermal alteration has occurred, probably due to the thermal effects of the impact event.

In addition to textural data from the SEM, microprobe and X-ray diffraction were used to determine the nature of alteration minerals in the Lonar samples. The microprobe results suggest that the majority of the clay materials in the Lonar samples are saponites and celadonites. Both saponite and celadonite are produced during the hydrothermal alteration of basalt, typically at temperatures of 130-200°C. The production of these "hydrothermal" clays at Lonar was further established through geochemical modeling of the alteration process, and by stable isotope analysis.

Limits to hydrothermal activity in terrestrial craters: The presence of hydrothermal alteration at the Lonar crater can be used to suggest that Lonar is near the lower heat limit for generating hydrothermal processes, thus establishing a new lower size limit of 1.8 km diameter for impact-induced hydrothermal activity. A hydrothermal system has been documented in the somewhat larger 4 km diameter Kärdla impact crater [4]. In contrast, no evidence of hydrothermal activity has been found in the smaller 1.13 km diameter Pretoria Saltpan (Tswaing) crater [5], or in the 1.2 km diameter Meteor Crater in Arizona [6]. This information can be used to imply that small martian craters greater than one or two kilometers in diameter may also have the potential to form hydrothermal systems, as long as water was present in some form.

Implications for Mars: Hydrothermal alteration is important for trapping fluids, such as water in the subsurface of Mars, and for releasing material to the surface. As a preliminary example, the amount of water that could be trapped due to alteration of craters in the size range from 2 to 11 km in diameter can be calculated. Assuming an average depth of alteration of 400 m, a degree of alteration of 3% based on the average of our SEM feature scan determinations, a volume of altered material equivalent to a global layer of 2.8 m will be formed over martian history. Assuming a water content of 10 wt% (e.g. similar to the amount in Lafayette martian meteorite iddingsite alteration material) this amount of material could trap an amount of water equivalent to a global layer of water 0.7 m deep. The one-meter value compares to estimates of the amount of water on Mars ranging up to a few hundred meters. In contrast Griffith and Shock [7] estimated that 8% alteration of 10% of the Martian crust could trap 30 m global equivalent of water.

References: [1] Newsom et al., (2001) *Astrobiology 1* 71. [2] Fredriksson, K. et al. (1973) *Science, 180,* 862. [3] Hagerty and Newsom (2003) *JGR* submitted. [4] Kirsmäe K. et al., (2002) *MAPS 37*, 449-457. [5] Brandt D. AND Reimold W.U. (1999) *Memoir 85* Council for Geoscience, Geological Survey of South Africa, 6-34. [6] Hörz F., et al (2002), *MAPS, 37*, 501-531. [7] Griffith L. L., and Shock E. L. (1997) *JGR 102*, 9135-9143.

ANTIPODAL HOTSPOTS ON EARTH: ARE MAJOR DEEP-OCEAN IMPACTS THE CAUSE? J. T. Hagstrum, U. S. Geological Survey, 345 Middlefield Road, MS 937, Menlo Park, CA 94025, jhag@usgs.gov

Introduction: Hotspot volcanism on Earth is restricted to relatively small areas, on the order of 100 km in diameter, and is generally believed to result from narrow upwellings of hot mantle material called 'plumes'. At first glance, hotspots appear randomly distributed. General associations with geoid highs and divergent plate margins have been noted [1], and hotspots tend to occur in provinces separated by spotless areas [2]. Matyska [3] investigated angular symmetries of hotspot distributions, and showed that the highest maxima were obtained with 180° rotations. Rampino and Caldeira [4] also conducted a statistical analysis of large and small data sets and found that more hotspots occur as nearly antipodal pairs than would be expected from random distributions.

The rise of antipodal plumes from the core-mantle boundary through a convecting mantle seems unlikely, but axial focusing of an impact's energy by the spherical Earth might underlie the antipodal pairing of hotspots [5, 6]. Such a focusing mechanism has been proposed to explain seismically disrupted terrains antipodal to major impact basins on the Moon and Mercury [7], and to explain formation of fractured crust on Mars opposite the Hellas basin—perhaps later exploited as a conduit for volcanism at Alba Patera [8]. First-order problems with this model for Earth, however, include the expected low seismic efficiency of impacts [7] and the lack of any volcanic features opposite large continental impact structures (e.g. Chicxulub).

Antipodal Hotspots: Although as many as 122 hotspots have been proposed [9], the number most commonly discussed is between 40 and 50. In a recent compilation of hotspots (plus 3) totaling 52 [10], 30 form antipodal pairs (~58%) with angular distances ranging from 168° to 179°. Deviations from 180° might be explained by an observed drift rate between hotspots of ~10 to 20 mm/yr [11].

One test of antipodal formation due to impact and focusing of seismic waves is to determine whether hotspots of a given pair began simultaneously. Tectonic recycling of oceanic crust, however, has made this impossible for most of the older pairs. For a few younger hotspot pairs, estimated initiation ages are roughly contemporaneous. Both Aitu (Cook Islands) and Tibesti (175°) are Late Miocene in age; Kerguelen and the Columbia River basalts (Yellowstone; 175°) are Early Miocene in age; the Marquesas hotspot track and Ethiopian flood basalts (Afar; 179°) are ~30 Ma in age; and the Balleny track indicates an age >40 Ma consistent with Iceland's (178°) age of ~55 Ma.

Individual hotspot pairs can generally be divided between one associated with initial flood basalts and rifting (e.g. Afar), and the other with oceanic affinities and no flood volcanism (e.g. Marquesas). It is hypothesized that the oceanic hotspots represent impact sites and those associated with voluminous volcanism the antipodal sites. Moreover, the geographic distribution of a large (122) hotspot compilation [9] shows that hotspot provinces are generally opposite oceans and that spotless areas are opposite continents [2].

Deep-Ocean Impacts: If these observations are correct, what process would cause oceanic impacts to form hotspot pairs, and continents to apparently shield their formation? A significant difference between continental and oceanic impacts is the formation of a high-pressure steam cloud above the oceanic impact site [12]. The pressure of the steam cloud might 'cap' the explosive release of energy from the seafloor impact, causing significantly more energy to be directed downwards.

A simple analog of deep-ocean impacts might be the surface blasting technique for secondary rock breaking known as 'mudcapping'. Mudcapping works due to the impulse action of explosives, which is proportional to the detonation pressure and its time of application on a rock burden [13]. A mudcap maintains the impulse pressure over a longer period of time, and the coupling effect depends partly on the amount of mudcap being used. In contrast, in a continental impact much of the energy released is likely directed upward and away from the land surface, resulting in a much lower seismic efficiency.

Conclusions: Although few impacts in the deep oceans are known, these events might have important consequences in the formation of hotspots, flood basalt provinces, and the breaking up of continental masses on Earth. Moreover, oceanic impacts, megatsunami waves, and antipodal continental flood basalts could be a major cause of global mass extinctions, and could explain rapid sea-level and abrupt ocean chemistry changes at extinction boundaries. Few models of deep-ocean impacts have been made, and it is suggested that a needed modification is the consideration of pressure effects from the steam cloud above the site upon energy release from the seafloor impact below.

References: [1] Jurdy and Stefanick (1990) *GRL*, *17*, 1965-1968. [2] Vogt (1981) *JGR*, *86*, 950-960. [3] Matyska (1989) *EPSL*, *95*, 334-340. [4] Rampino and Caldeira (1992) *GRL*, *19*, 2011-2014. [5] Hagstrum and Turrin (1991) *Eos*, *72*, 516. [6] Boslough et al. (1996) *GSA Spec. Pap. 307*, 541-550. [7] Schultz and Gault (1975) *The Moon*, *12*, 159-177. [8] Williams and Greeley (1994) *Icarus*, *110*, 196-202. [9] Burke and Wilson (1976) *Sci. Am*., *235*, 46-57. [10] Courtillot et al. (2003) *EPSL*, *205*, 295-308. [11] Molnar and Stock (1987) *Nature*, *327*, 587-591. [12] Melosh (1982) *GSA Spec. Pap. 190*, 121-127. [13] Cook (1958) *Am. Chem. Soc. Monogr*., *139*, 278-279.

MAGNETIC FIELDS OF LUNAR IMPACT BASINS AND THEIR USE IN CONSTRAINING THE IMPACT PROCESS.
J.S. Halekas, R.P. Lin, *Space Sciences Laboratory, University of California, Berkeley CA 94720 (email: jazzman@ssl.berkeley.edu).*

Measurements by the Magnetometer/Electron Reflectometer instrument on the Lunar Prospector spacecraft, which completed its mapping mission in 1999, have been used to construct the first completely global maps of lunar crustal magnetic fields. Now, for the first time, we have a data set with global coverage and a sensitivity and resolution which allow us to investigate the magnetic fields of lunar impact basins and craters. As on the Earth, impact sites have a variety of magnetic signatures associated with them, ranging from nearly complete demagnetization to strong central magnetic anomalies. Observations of the magnetic fields of terrestrial basins have been used to make inferences about the impact process, and we wish to show that lunar observations can also provide valuable constraints.

It is clear that we can not achieve the same kind of magnetic field data coverage of lunar basins with measurements from orbit that we can for terrestrial basins using ground magnetometer or aeromagnetic data. Furthermore, lunar missions have only returned a limited number of samples of actual magnetized crustal rocks, while on the Earth we can study as many samples as one could wish. Therefore, one might wonder why lunar data should be used at all, when terrestrial data has these clear advantages. However, the Moon has several key advantages over the Earth for this type of study. First and foremost, the Moon currently has no global magnetic field. This means that we do not have to subtract off a huge global field when measuring local crustal fields, nor do we need to deal with induced magnetic fields. Instead, we can be sure that the signal we measure is purely due to remanent magnetization in the local crustal rocks. Furthermore, on the Earth impact basins formed in the presence of a strong ambient magnetic field. On the Moon, on the other hand, at least the younger basins and craters appear to have formed with no significant ambient magnetic field present. This means that we can more easily determine the demagnetization effects of these impacts.

Studies of terrestrial impact basins have revealed many basin-associated magnetic anomalies [1]. These range from short-wavelength anomalies with a radial extent of a fraction of the transient cavity radius (e.g. Manicougan [2]), to larger groups of anomalies which fill most of the transient cavity region (e.g. the outer ring of anomalies in the Chicxulub basin [3]). The more localized anomalies have generally been ascribed to shock remanence (SRM) or other processes in the central uplift region, while more extensive anomalies have been interpreted as thermal remanent magnetization (TRM) in impact melt rocks. Many lunar basins and craters also display central magnetic anomalies, with the older large (> 200 km in diameter) craters and basins having the most significant anomalies. These anomalies roughly fill the transient cavity region, and therefore by analogy with terrestrial basins, may be due to TRM in impact melts. If this is the case, these anomalies indicate the location of the most substantial amounts of impact melt in lunar basins. On the other hand, if they are instead due to SRM in uplifted materials, they could be used to delineate central uplift structures in multi-ring basins.

Earlier work has shown that many lunar impact craters and basins, especially the youngest ones, are demagnetized with respect to their surroundings [4]. This is also true of many smaller terrestrial craters [1,5]. However, for younger lunar impact sites, demagnetization is especially clear, probably because there were no strong ambient magnetic fields present at the time of these impacts. The demagnetization of lunar craters and basins has been found to extend well beyond the main rims of these structures, which provides strong evidence that impact-generated shock is mainly responsible for demagnetizing the crustal rocks [4].

The physical mechanism of shock demagnetization is still not particularly well understood. However, laboratory measurements of shock demagnetization of both lunar and terrestrial rocks have been performed [6,7,8]. The degree of demagnetization is, in general, dependent on the peak shock pressure and on the remanent coercivity of the crustal magnetization, and laboratory experiments have roughly quantized this relationship for terrestrial basalts [6]. The returned lunar samples show a wide variety of magnetic coercivity spectra. However, lunar breccias tend to carry the strongest remanence, and we have therefore constructed average coercivity spectra for various sets of breccias [9,10]. By combining coercivity spectra with impact demagnetization data and experimental shock demagnetization results, we have attempted to derive the radial peak shock pressure attenuation. Our preliminary results imply peak shock pressures at the transient cavity rim of 2 Gpa and power law attenuation with a power of -2 to -3. These results are consistent with modeling [11] and shock pressure reconstructions from terrestrial basins [12].

We believe that the magnetic fields of lunar impact craters and basins can provide important information about the impact process. Though performing this work with lunar rather than terrestrial data has some drawbacks, there are also clear advantages. So far, our results are encouragingly consistent with terrestrial observations and modeling.

REFERENCES: [1] Pilkington and Grieve, *Rev. Geophys., 30*, 161-81, 1992. [2] Coles and Clark, *J. Geophys. Res., 83*, 2805-8, 1978. [3] Pilkington and Hildebrand, *J. Geophys. Res., 99*, 13147-62, 1994. [4] Halekas *et al., Geophys. Res. Lett., 29, 10.1029/2001GL013924*, 2002. [5] Scott *et al., Meteorit. Planet. Sci., 32*, 293-308, 1997. [6] Pohl *et al., J. Geophys., 41*, 23-41, 1975. [7] Cisowski and Fuller, *J. Geophys. Res., 83*, 3441-58, 1978. [8] Cisowski *et al., Proc. Lunar Planet. Sci. Conf., 6*, 3123-41, 1975. [9] Gus'kova *et al., Cosmic Research, 12*, 680-8, 1974. [10] Fuller, *Rev. Geophys., 12*, 23-70, 1974. [11] Ahrens and O'Keefe, in *Impact and Explosion Cratering* ed. Roddy, Pepin, and Merrill, 639-56, 1977. [12] Robertson and Grieve, in *Imp. and Exp. Crat.*, 687-702.

PYROCLAST FLOWS AND SURGES: POSSIBLE ANALOGY FOR CRATER EJECTA DEPOSITION. H. Hargitai[1], A. Kereszturi ([1]Dept. of Physical Geogr., Email: hargitai@emc.elte.hu, Dept. of Physical and Historical Geol., Eötvös Loránd University of Sciences, H-1083 Budapest, Ludovika tér 2., Email: krub@freemail.hu)

Introduction: We analyse a possible modell of the crater ejecta development and deposition with pyroclastic flows and surges. Because several of their characteristics and depositional structures are known and observable on the Earth it is useful to try to find resembling phases of the crater ejecta formation.

The modell: We analyzed similarities and differences of physical parameters between pyroclastic flows and crater ejecta formation. At volcanic eruptions the p, T are lower than at the moment of impact. In the origin of the pyroclastic flows we can analyse the physical circumstances at really explosive eruptions like Krakatoa-type eruptions too. The 1st seconds of the impact – contact/compression stage (CC), the kinetic energy is transfered to the rock by schock waves. In our analogy we ignore this phase because the differences are too large. The original energy is lost fast because of the expanding shock front and the conversion of the energy to heat, rock deformation etc. When the pressure drops to 1-2 GPa it behaves like normal seismic waves. [1] Heat melts the projectile and target rock layers, which is mixed to partly melted and brecciated target rocks.

At the end of the excavation stage [E] the ejecta material (the near surface ejecta curtain) falls out of the rim of the crater and its material flows away and settles down. At pyroclastic flows and surges originally high central pressure formed the fragments which later was transported by gravity at slopes. At a crater formation the impact explosion gas schock waves, reflected waves drive the upward movement of the debris. We can use the analogy at that point where the effect of the central pressure is lower and gravity driven current movement is important. Our analougue is best in the modification [M] stage when the transient crater reached its final dimensions and no more material is ejected. The ejecta blanket is now "in the air" and starts falling down. From this point the physical parametrs of this material is more or less similar to the ones in a volcanic eruption. By this time, the crater rim is higher then the surroundings so there is a slope corresponding to a volcanic dome that makes the flow movement possible.

In pyroclastic structures several distinct layers are identifiable. A crater ejecta structures can be taken as one cycle of a pyroclastic structure. The cratering process is ended after the solid materials fell down, with the finer particles gravitational settleing and the fallout of the solidified materials that were vapourized during the impact. The resulting distal ejecta can be extended to a global scale. These later stages are also analogues to the volcanic eruptions.

Characteristics	Pyroclastic flows	Pyroclastic surges	Crater ejecta emplacement
Temperature	900-1100 K and lower	900-1100 K and lower	1000-2000 K and lower
Pressure	first in the order of Mpa, later near to the atmospheric	firstly in the order of MPa, later near to the atmospheric	first [CC] in the order of GPa, later [M] nearly near to the atmospheric
Fragments	Mostly solid with gas and very few liquid phase	large gas content with lower solid matter ration	Solid phase and gas, with more plastic components (melts) Melts from projectile/target; solid rocks from target area, vapourized gas from projectile/target
Depositional structures	Poorly sorted and bedded, graded basal zone, trains of large fragments, alternating coars to fine graded layers, oriented fragments, at pumice inverse grading	laminated, cross bedding, lenses of well-sorted-rounded pumice lapilli, better sorted, no very fine and very coarse fractions	Fallout partly influenced by flowing movements
Driving force	gravitational induced movement on slopes	gravitational induced movement on slopes	first the gas pressure of the explosion [E], later gravitational induced motion on slope
Topography	relative high slope angle	relative high slope angle	nearly no originally slope, only in the late phase of the deposition low slope angle (from the rim)
Origin	collapse of the ejecta containing (simetimes km high) gas column above the central vent	mostly explosion driven fallout of ejecta, and later the collapsa of shorter gas driven explosion column	fallout (ejecta) from the central explosion
Duration of material upload	several hours/days?		Few seconds
Source of gas content	eruption column; outgassing of melt	eruption column; outgassing of melt; water of crater lake	vapourized projectile (if comet, more) or rock, in situ ground- or surface water or ice; outgassing of melt; On Venus: atmosphere
Speed	ejected material: 200-600 m/s; flow: 100-200 km/h	flow: 100-200 km/h	ejected material: 500 to several 1000 m/s

Comparison of flows, surges, crater ejecta

It is a question whether there is an eruption column at the impact site. In the case of volcanoes, the eruption column is supported by the continuos gas thrust from the crater which is not the case at impacts where the process takes place for few seconds. Observations of nuclear explosion tests show both eruptive coloumns and gasious flows just like surges too. [3] The ejecta blanket is partly fluidized by water.

The atmosphere is important with its pressure for the gas content inside the pyroclastic flow. At the crater ejecta in the depositional phase the difference between the atmospheric and the internal pressure is relative low – just like at a pyroclastic flow. Because pyroclastic structures are known from airless body our analogy can be used at the crater ejecta deposition on airless bodies, eg. on moons. Higher gas content cab make fluidization. On Venus, the long-run ejecta flows were spread in a fluid manner, extending beyond the continous ejecta, moving on a fluidized "bed" which are linked to impact melts, impact angle [2] and dense atmosphere.

Conclusion: In the late phase of the crater ejecta formation pyroclastic flows can be used as an analogy in the analysis of physical circumstances in the flow (flow regime, temperature, gas content, ration of liquid phases). The depositional structures can suggest to the density of the debris and fallout style/time.

References: [1] B.M. French: Traces of Catastrophe LPI Contribution No. 954. [2] W.B. McKinnon et al. (1997): Cratering on Venus: Models and Observations in Venus II. Geology, Geophysics, Atmosphere, and Solar Wind Environment. UAP. [3] J.G. Moore (1998): Base surge in recent volcanic eruptions. Bull. Volc. 30, 337-363, ref. in: D. Karátson: Volcanology. ELTE.

THICKNESSES OF AND PRIMARY EJECTA FRACTIONS IN BASIN EJECTA DEPOSITS. Larry A. Haskin and William B. McKinnon, Department of Earth and Planetary Sciences and McDonnell Center for the Space Sciences, Washington University, One Brookings Drive, St. Louis, MO 63130; lah@levee.wustl.edu, mckinnon@levee.wustl.edu

We have developed a model for production of basin ejecta deposits to address provenances of materials collected at the Apollo and Luna landing sites and for consideration in interpreting remote sensing data [1].

Model Steps: **1)** We take the cumulative mass (m) distribution of primary ejecta fragments ("PriFrags") to vary as $m^{-0.85}$ everywhere, with a maximum PriFrag mass (which can vary with ejection velocity) [e.g., 2, p. 91]. **2)** Ejecta mass is distributed according to [3]. We map their results, for a flat surface, onto a spherical one using ejecta velocities and an assumed launch angle. **3)** Given the surface density of PriFrags of each size falling in the vicinity of the site of interest, we use Schmidt-Holsapple scaling to obtain the sizes of secondary craters. We assume *excavated* volumes of those craters have a depth/diameter ratio of 0.1. **4)** We calculate the probable range of ejecta deposit thickness and % of PriFrags in the deposits, and express them as the fraction of the area at the site of interest. We define "Coverage Level" (CL) as the fraction of that area excavated by craters of a specific size *or larger*. **5)** Beginning with the cavity produced by the largest PriFrag to excavate at a location, we consider how much additional substrate is excavated by the smaller PriFrags that land on or near that spot. We calibrate to deposit thicknesses surrounding Orientale [4] and the Ries [5]. Results suggest that the total excavation by all secondary craters at a specific position corresponds roughly to a right cylinder with the same diameter and 3 times the depth of the largest crater to affect that position.

General Model Results: Ejecta deposit thickness decreases with distance to ~3500 km followed by a modest increase on the anti-basin hemisphere due to ejecta convergence. The fraction of PriFrags in the ejecta deposits shows a similar pattern. Differences due to varying ejection angle from 35° to 55° (to the horizontal) are not substantial.

Apollo 16 Landing Site: Fig. 1a shows the range of deposit thicknesses expected in the vicinity of the Apollo 16 site ~1600 km from the center of Imbrium. Thickest deposits are produced where the largest PriFrags excavate; at higher coverage levels, relatively smaller PriFrags have excavated. Locations where different deposit thicknesses occur are not known, as the impact points of all PriFrags are random. Thus, some half of the vicinity of the site has ejecta deposits ≥1 km or so. From Fig. 1b, the fraction of PriFrags in the deposits is not sensitive to coverage level.

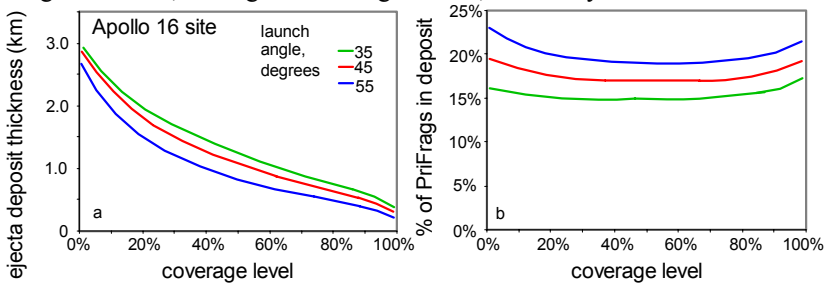

Fig. 1. a) Ejecta deposit thickness vs. coverage level for launch angles of 35°, 45°, and 55°. b) % of PriFrags in deposit vs. coverage level.

Estimated deposit thicknesses at the Apollo 16 site are reasonable as determined by criteria such as crater fill and fraction of Th-rich ejecta presumed delivered to the site by the Imbrium event from the Procellarum KREEP Terrane [6]. In contrast to conclusions of other studies [7,8], our modeling suggests that all materials sampled at the site, including North Ray Crater ejecta, are more likely part of the Imbrium deposit than part of a primary Nectaris deposit. The Imbrium deposit is estimated to consist of 18% Imbrium ejecta, 21% Serenitatis ejecta, 19% Nectaris ejecta, and 40% pre-Nectarian substrate, with only minor contributions from Humorum, Crisium, and later, Orientale. These materials may not be well mixed; large blocks from different provenances could presumably survive in some locations. The presence of significant Serenitatis materials at the Apollo 16 site has been discounted owing to lack of compelling photogeologic evidence [9, Fig. 10.39; 10, Fig. 10.25].

Concerns: Our model does not reproduce observed densities of secondary craters (it predicts too many) or the largest ones at Copernicus, Orientale, or Imbrium. Mutual obliteration and contributions from "spall" fragments may be responsible, respectively [cf. 11]. Nevertheless, thick deposits should have been produced at great distances from basin impact sites, and these deposits should consist of mixtures of primary ejecta and megaregolith produced by previous large impact events. How thick, however, depends on scaling parameters and factors that are still poorly known. These will be discussed. This work supported by NASA grant NAG5-10458.

References: [1] HASKIN ET AL. (2003) *MAPS*, in press; [2] MELOSH H.J. (1989) *Impact Cratering*, Oxford; [3] HOUSEN ET AL. (1983) *JGR* **88**, 2485–2499; [4] MOORE ET AL. (1974) *Proc. LPSC* **5th**, 71–100; [5] HÖRZ, F. ET AL. (1983) *Rev. Geophys. Space Phys.* **21**, 1667–1725; [6] JOLLIFF B. L. ET AL. (2000) *JGR* **105**, 4197–4216; [7] SPUDIS P. D. (1993) *The Geology of Multi-Ring Impact Basins*, Cambridge; [8] STÖFFLER D. ET AL. (1985) *JGR* **90**, suppl. C449–C506; [9] WILHELMS D. E. (1987) The Geologic History of the Moon, *USGS Prof. Paper* **1348**; [10] SPUDIS P. AND PIETERS C. (1991) in *Lunar Sourcebook*, G. Heiken et al. (eds.) Cambridge; [11] VICKERY A. M. (1987) *GRL* **14**, 726–729.

CONSTRAINTS ON THE IMPACT PROCESS FROM OBSERVATIONS OF OBLIQUE IMPACTS ON THE TERRESTRIAL PLANETS. R. R. Herrick and K. Hessen (Lunar and Planetary Institute, 3600 Bay Area Blvd., Houston, TX 77058; Herrick@lpi.usra.edu).

Introduction: Recently there have been significant advances in both experimental and numerical modeling techniques that hold promise for providing details on how the cratering process is affected by impact at a nonvertical angle [1,2]. Anectdotal observations of craters on the terrestrial planets validated initial experimental efforts [3,4]. Recent and ongoing systematic characterizations of craters reslting from oblique impact on the Moon, Mars, and Venus provide important constraints for the detailed modeling efforts currently being conducted [5,6,7].

Observations: Pertinent observations from surveys conducted to date are:

- The general variation in ejecta pattern and crater shape with decreasing impact angle on the moon matches well with experimental work conducted in a vacuum. On the moon the following transitions occur with decreasing impact angle with respect to horizontal: < ~50 degrees, the ejecta blanket becomes asymmetric; < ~30 degrees, a forbidden zone develops in the uprange portion of the ejecta blanket, and the crater rim is depressed in that direction; < ~20 degrees, the rim topography becomes saddle-shaped, or depressed in both uprange and downrange directions; < ~15 degrees, the rim becomes elongated in the direction of impact and the ejecta forms a "butterfly" pattern in the crossrange direction [5].
- In agreement with experimental work, the presence of an atmosphere significantly increases the onset angle of oblique impact phenomena in the ejecta pattern [5]. No downrange forbidden zone occurs at low impact angles [4].
- Our preliminary work with Martian craters shows that the change in ejecta pattern with decreasing impact angle closely resembles that of the moon, with the development of uprange and then downrange forbidden zones with decreasing impact angle. While the transition angles to different ejecta patterns are generally similar on the moon and Mars, the development of a forbidden zone in the uprange direction occurs at a significantly higher impact angle on Mars than the moon.
- The transition to elliptical craters and a butterfly ejecta pattern occurs at a higher angle on the planets than in early experimental work [3,5,6].
- Adequate data on crater wall topography of oblique impacts currently only exist for the moon. Unlike in experimental work, there is no strong evidence of uprange steepening of the crater wall for oblique impacts [5]. Internal slopes for lunar craters appear largely independent of impact angle. However, interior crater wall slopes approach the angle of repose, and post-impact slumping to a uniform slope cannot be ruled out.
- There is minimal evidence that central structures are offset in any direction relative to the crater rim [7], nor could we find observations in imagery that were indicative of the point of impact.

Constraints on the Impact Process: The observations suggest the following constraints on modeling efforts of the impact process:

- That the ejecta pattern is more affected by oblique impact than the final crater shape suggests near-field versus far-field effects; material ejected from near the point of impact "sees" the impact angle the most.
- Modeling of ejecta emplacement in an atmosphere must consider the disturbance of the atmosphere by the incoming projectile.
- Whatever causes the higher onset angle for elliptical craters and butterfly ejecta on the planets relative to past experimental work, those causes are only important at the lowest impact angles.
- The lack of variation for interior shape and slope suggests that the cross-section of stream tubes for late-stage excavation does not vary with impact angle.
- Mars is clearly below the threshold for the atmospheric disturbance caused by the incoming projectile to have a significant effect on ejecta emplacement.
- While subsurface features may reflect the initial point of impact, observable surface features do not. In other words, while the shock level of the rocks can be modeled as strongly direction-dependent, final crater shape must not be (with exception of rim elevation).

References: [1] Pierazzo E. and Melosh H. J. (2000) *Ann. Rev. Earth Plan. Sci., 28,* 141-167. [2] Schultz P. H. et al. (2000) *LPS XXXI,* Abs. #1902. [3] Gault D. E. and Wedekind J. A. (1978) *Proc. LPSC 9th,* 3843-3875. [4] Schultz P. H. (1992) *JGR, 97,* 16,183-16,248. [5] Herrick and Forsberg (2002) submitted to *Met. and Plan. Sci.* [6] Bottke W. F. et al. (2000) *Icarus, 145,* 108-121. [7] Ekholm A. G. and Melosh H. J. (2001) *GRL, 28,* 623-626.

LINKING EXPERIMENTAL MODELLING OF IMPACT CRATERS TO STRUCTURAL COMPONENTS OF THE REAL THING. A. R. Hildebrand[1], [1] Department of Geology and Geophysics, 2500 University Drive NW, University of Calgary, Calgary, AB T2N 1N4 (hildebra@geo.ucalgary.ca)

Introduction: Impact crater scaling relationships, such as for impact energy, are usually derived solely from experimental impact or explosion craters [e.g., 1]. Relating craters to a suite of possible source projectiles, and predicting what size crater a given impactor will produce in a surface of known composition, are basic requirements for reconstructing impactor populations from cratering records, comparing cratering rates derived from cratering records to those derived from observed impactor populations (known velocities), and assessing the hazard associated with a given impactor.

Impactor to Crater Size/Energy: Scaling from a given crater to impact energy is currently controversial even when the same energy scaling relationship [e.g. 2] is used. For example, energy estimates for the Chicxulub crater [3,4] vary by an order of magnitude due to interpretation differences, although agreement exists on the relevant internal crater structural element (the collapsed disruption cavity diameter; see Fig. 1). (Discussion indicates that confusion exists within the cratering community on terminology for the different crater elements illustrated in Fig. 1; agreement on a common terminology as discussed by [3] is desirable.) The difference stems from one calculation being based on the reconstructed size of D_d [4] and one being based on D_{at} [3]. The latter have been convinced by the argument (p.c., H. Melosh) that the apparent transient cavity diameter corresponds to that of the experimental craters produced by [2] on the grounds that no collapsed blanket of breccia or melt fills the craters.

Possible Link Through Ejecta Blankets: The appropriate cavity diameter to be used for energy scaling might be established by comparing the ejecta blanket thicknesses observed around Chicxulub to those around experimental craters. Figure 2 attempts this comparison (the ejecta thicknesses are plotted normalized to a D_{at} of 80 km [3]). However, sufficient observations are not yet available to make a clear distinction, and erosion by ballistic sedimentation proximal to Chicxulub has over thickened its ejecta blanket by nearly an order of magnitude (as also observed around other well preserved craters). Although the thickness of the proximal ejecta blanket has also been compromised by erosion of its top, comparison of the observed thickness to that predicted from experimental craters may be useful in predicting the proportion of the ejecta blanket that is derived from ballistic erosion. At >15 crater radii observed ejecta blanket thicknesses are greater than predicted by [1, Fig. 2], this range is beyond the thickness resolution of these experiments.

References: [1] Housen, K.R., Schmidt, R.M. and Holsapple, K.A. (1983) *JGR, 88,* 2485–2499. [2] Schmidt, R.M. and Housen, K.R. (1987) *Int. Jour. Imp. Eng., 5,* 543-560. [3] Hildebrand, A.R. et al. (1998) *Meteorites: Flux with Time and Impact Effects, Geol. Soc., London, Spec. Pub. 140* 155–176. [4] Morgan, J. et al. (1997) *Nature 390,* 472-476.

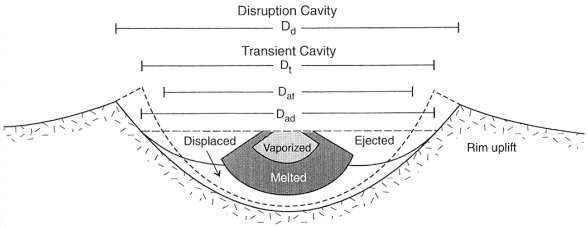

Figure 1: Schematic distinguishing a crater's transient (diameter D_t) and disruption (diameter D_d) cavities. At the pre-impact ground surface these diameters are D_{at} and D_{ad}, respectively. The horizontal dashed line indicates the position of the pre-impact surface within the crater. (from [3])

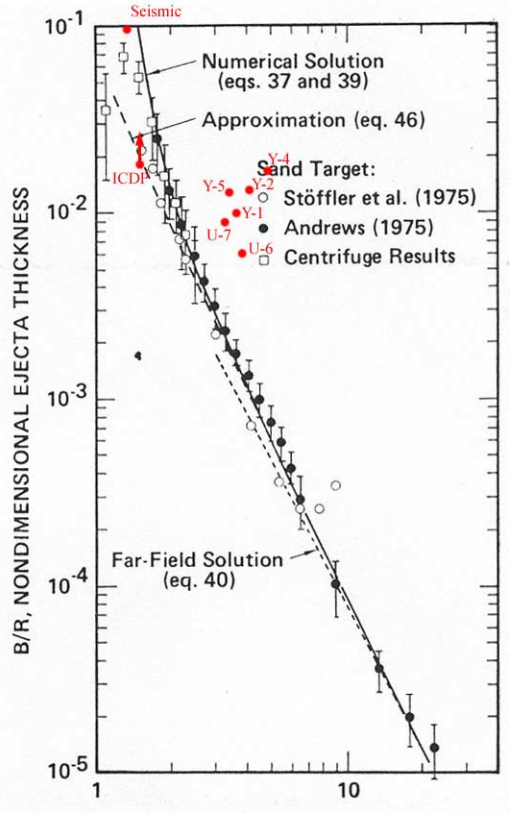

Figure 2: Ejecta-blanket profiles resulting from experimental impacts and explosions in sand compared to profiles predicted by the ejecta model of Housen et al. [1] and the ejecta blanket thicknesses observed at the Chicxulub crater. (Modified from [1])

WHAT DO WE NEED TO KNOW TO MODEL IMPACT PROCESSES?

K. A. Holsapple, University of Washington, 352400, Seattle, WA 98195. holsapple@aa.washington.edu.

Introduction. The computer modeling of hypervelocity impacts into planetary bodies is one of the most challenging computer tasks we attempt. The physical states encountered in impact events can begin with pressures measured in gigabars and temperatures measured in hundreds of electron-volts, and then proceed all the way down to the ordinary partial bars of pressure and few degrees of temperature as in our common experience in terrestrial soils and rocks. The interest in planetary science applications spans not only those common terrestrial soils and rocks, but also gases, ices at extreme low temperatures, and very loose, rubble-pile materials that could not even withstand the pressures of the Earth's gravity without crumbling.

The extreme range of physical conditions and materials makes the job of a modeler extremely difficult, especially for descriptions of the models for the material behavior. While, in principle, current computer power would seem to allow the detailed calculation of any specific impact event of interest by integrating the known physical laws, that view is specious. The cold, cruel facts are that, first, we do not yet know how to mathematically model the extreme range of conditions of importance, and second, even if we develop meaningful models, we do not have sufficient physical tests to measure the material properties needed for those models.

This state of affairs means that the community must be aware of the shortcomings, and must spend much more time and effort on the development of models of material behavior, on the laboratory and field measurements to calibrate those models, on calculations to determine the sensitivity of the results on the models, on actual physical experiments of impacts, and, finally, on calculations of those physical laboratory results and large scale field events with known impact conditions. The computer tools must prove their reliability and robustness for calculations when both the initial and final conditions are well known before they can be used with any meaning to determine unknown impact conditions.

This presentation is to review what we know and what we do not know; what needs to be known, and what remains to be discovered about material modeling for impacts.

The EOS. The evolution of the pressure and temperature states from extremely large to very small leads to a parallel separation of the required material models into two distinct but intertwined parts. First are the models for the high-pressure behavior in the early stages of the process. Those pressures are commonly much larger that the material stress scales: the compressibility modulus and various material strengths, so the stress deviators can be ignored. The state is then measured by five state variables: the pressure p, mass density ρ, internal energy e temperature T and entropy η. Any pair can be chosen as independent, and the other three are then given in terms of those two by the "equations of state" which are material property functions. However, insofar as the solution for the motion is concerned, it is only the relation between e, p and ρ that matters.

Since impact problems encounter the same extreme conditions as nuclear events, it is not surprising that we borrow the knowledge and tools of the national weapons laboratories for those equations of state, which they have been studying for over half a century.

There are a variety of EOS models: simple algebraic models that relate pressure and density with no dependence on temperature (e.g. linear elasticity or Murnaghan); simple analytical models for single solid phases (Mie-Gruneisen and Tillotson); complex analytical models including phase changes such as melt and vapor (ANEOS); and complete tabular databases such as the SESAME and SESLAN libraries from the DOE laboratories. Those latter two are often developed from complex solid-state physics theories using the PANDA computer code [1]. The EOS equations govern the early-time response and determine a number of significant aspects of the energy coupling, including the initial pressure and velocity, and the decay of the pressure and velocity as a shock propagates through the target.

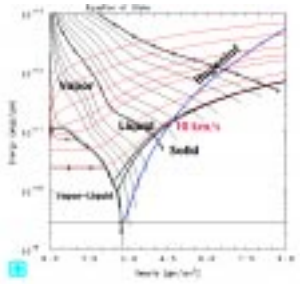

A typical EOS is as shown at the left. The important elements include the Hugoniot, which relates the conditions at the shock, and the "release adiabat" the path followed during the unloading behind the shock.

These paths determine a measure of an equivalent point source input, which in term determines most of the scaling of the final cratering or disruption results.

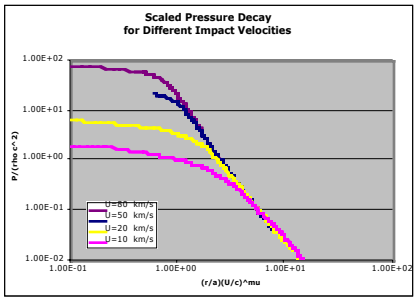

The left figure illustrates the commonality of different impact problems arising from the simplicity of the point-source measure. (See [2] and many prior references of the author

and his colleagues.)

These EOS descriptions are quite well developed and understood, a consequence of the fact that they are needed for calculations and development of nuclear weapons. For impact calculations, it is necessary to choose the model and its constants. However, for any particular geological material, that can often be a difficult task, so that the resulting model is usually quite uncertain.

Strength. When the shocks decay into the kilobar pressure range, material strength dominates the target response and subsequent cratering or disruption. Here we borrow from the civil engineering soil-mechanics and rock-mechanics communities.

Strength models include none (hydrodynamic), constant strength in tensile or compression, constant strength in shear (Tresca), maximum deviator invariant J_2 (VonMises), pressure-dependent shear strength (Mohr-Coloumb), pressure-dependent J_2 (Drucker-Prager), rate-dependent tensile (e.g. Grady-Kipp), and complex damage models (e.g. Johnson-Cook). This description of the fracture, flow or yielding (generically called "failure") is the most difficult part of impact calculations into geological materials.

A common starting point is to describe how the initial failure depends on the stress or strain tensors, which have six independent components; or, equally well, three invariants and three directions. Assuming isotropy, directions are of no consequence and the stress tensor can be measured by the three invariants. It is common to further suppose that only two are necessary, taken as the pressure or mean stress (essentially the first invariant), and what is commonly denoted by J_2 , the second invariant of the deviator stress. Then the ranges of stress for which flow or fracture does not occur are described by defining an enveloping curve in pressure-J_2 space. (Changes to this envelope such as hardening or softening are described below).

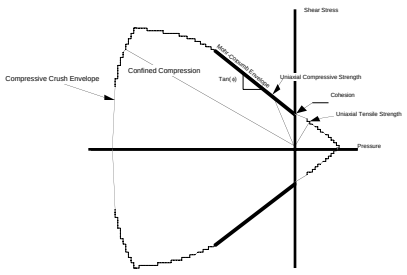

The figure at the left indicates the general nature of an initial failure envelope for a geological material, as a plot of the maximum shear stress versus the confining pressure. Various different measures of "strength" exist and are indicated on this envelope. There is a curve of limit shear stress that depends on pressure, commonly modeled as a Mohr-Coloumb (shear strength versus pressure) or a Drucker-Prager envelope (J_2 versus pressure). Often those curves are assumed to be linear, but that assumption is not essential. Then since failure can also occur at sufficiently high pure compressive pressure, a "cap" is constructed to model that compressive pressure crushing; that is the termination of the envelope at the left of this figure.

For uniaxial tension loading, the loading path as shown intercepts the failure envelope at a uniaxial stress limit known as the tensile strength. In pure uniaxial compression, the path as indicated intercepts the shear envelope at a higher stress, called the compressive strength. In pure shear, the maximum is at the intersection of the shear envelope with the vertical axis, the shear strength or "cohesion". Biaxial or triaxial loading can proceed along different paths until they intersect these limit curves, those define biaxial and triaxial strengths. A confined compression curve is shown sloped to the left and intersecting the compression cap.

The next part of the modeling concerns the question of the change of this envelope as failure proceeds. These questions involve the features of ductility (plastic flow) versus brittle (fracture or flaw growth). Commonly, brittle failure occurs at low values of confining pressure, especially tensile states; while ductile failure occurs at high values of confining pressure in compressive states. Ductile failure is modeled by describing how the material develops plastic strain (the "flow rule") and by how that flow affects the failure envelope (hardening or softening). Common metal-plasticity models include those effects. Brittle failure is commonly modeled using a "damage" parameter, which measures the internal damage of the material in a macroscopic way. It typically ranges from zero at no damage, to unity at complete damage. An equation describing its evolution as a function of the current stress or strain state is required to track its values at material points. The Grady-Kipp model is an example of a damage model for brittle tensile failure. All of these aspects can also depend on the temperature.

When failure occurs, a granular material also has a tendency to "bulk": an increase in volume and decrease in density at constant pressure. That can be suppressed by the pressure state, but then adds a component of pressure. Equally well, bulking is included if an associated flow rule is used with a pressure-dependent shear strength, since that flow rule has a component of dilation. The relative amounts of deviator and dilation can be adjusted by using a non-associated flow rule.

I will review various material property data and different models used in the community, and relate their features and failures to this overview picture.

References:

[1] Kerley G. I., "Users Manual for PANDA II: A Computer Code for Calculating Equations of State", Sandia Report SAND88-2291, 1991.

[2]Holsapple, K. A., "The Scaling of Impact Processes in Planetary Sciences", *Annual Reviews of Earth and Planetary Sciences* **21** pp333-373, 1993.

DOES MELT VOLUME GIVE THE SIGNATURE OF THE IMPACTOR?

K.A. Holsapple, University of Washington, 352400, Seattle, WA 98195. holsapple@aa.washington.edu.

1. Introduction. Many analyses of impact events attempt to solve an inverse problem: Given the result, what was the impactor? One common example is the use of careful measurements of impact melt with the hope of deducing the impactor size and velocity.

The approach is as follows. Suppose the amount of impact melt is, for a given geological site and assuming a given impactor material, known (for example by code calculation) as a function of impactor mass m, velocity U. (I shall ignore complexities of oblique impacts here.) Then we have some known functional relationship

$$V_{melt} = F(m,U) \tag{1}$$

Then also we have some other known quantity, say the crater size given as

$$V_{crater} = G(m,U) \tag{2}$$

The goal is then to solve these two equations in two unknowns for the impactor mass m and the velocity U. Of course, that will fail if the two equations are not independent, and therein often lies the problem.

Equation (2) for the crater size is usually assumed to be of the form determined by the point-source approximation to impact problems, as given by the scaling relations of Holsapple, Schmidt and Housen (see, for example, the review in Holsapple 1993 [1]). The point-source approximation is expected to be valid for any measure of the cratering process that is large compared to the impactor size. Those relations have the form

$$V_{crater} = f\left(aU^{\mu}\right) \tag{3}$$

where the exponent m is assumed to be known, it is about 0.55-0.6 for non-porous materials. One must distinguish between the strength regime or the gravity regime for the function f. Assuming as a specific example a large terrestrial crater in a hard rock geology, then a specific form is given (Holsapple, 1993 [1]) as

$$V_{crater} = 0.48 m^{0.78} U^{1.3} \tag{4}$$

Thus, the measurement of the crater volume gives the numerical value for the product $mU^{1.67}$. (This is just the cube of the product aU^{μ} with some factors thrown in.)

We cannot perform laboratory experiments at impact velocities greater than 5-6 km/s, well below the minimum velocity for melt production. Therefore, code calculations must be used to determine the melt volume function of equation (1). Such calculations have been reported by O'Keefe and Ahrens [2], Orphal et al. [3] Bjorkman and Holsapple [4], Pierazzo et al. [5] and others.

O'Keefe and Ahrens [2] report that the melt volume for impact velocities greater than a threshold is proportional to the impactor kinetic energy:

$$V_{melt} = Ka^3U^2. \tag{5}$$

Later, Bjorkman and Holsapple [3] determined an importantly different result: that, for impact velocities greater than about 50 km/sec the melt volume scaled in the same way as the crater volume, namely that

$$V_{melt} = Km^{0.78}U^{1.3}. \tag{6}$$

although energy scaling does hold for lower velocities where the majority of melt is produced close to the impactor. The problem then arises for the larger velocities: if the melt and crater volumes scale in exactly the same way, both are determined by the same combination $mU^{1.67}$. Then there is no way to determine separately the mass and velocity.

Much more recently Pierazzo et al. [5] revisited the question of melt production. Their conclusion returns to that of O'Keefe and Ahrens: that the melt volume scales linearly with the energy of the impactor. They attribute the Bjorkman and Holsapple [3] result to be a consequence of insufficient grid resolution in the calculations.

I shall reevaluate the reevaluation of Pierazzo et al. Specifically, I shall show calculations and argue that, not only does energy scaling not hold for the higher velocities, it does not hold about 30 km/s. The consequence is that melt volume cannot be used to separate the effects of size and velocity for any impact velocity greater than that value.

In fact though, the different interpretations are really somewhat moot. Numerical examples will be presented that show, that even if energy scaling for melt volume is adopted down to lower velocities, the inverse problem is highly non-robust: Factors of uncertainty of only 2 in the melt or crater volume functions result in factors of uncertainty of several decades in impact velocity.

References:

[1] Holsapple, K.A., "The Scaling of Impact Processes in Planetary Sciences", *Annual Reviews of Earth and Planetary Sciences* **21** pp333-373, 1993.

[2] O'Keefe J.D. and Ahrens T.J. "Impact induced energy partitioning, melting, and vaporization on terrestrial planets." *Proc. Lunar Planet. Sci. Conf, 8th*, 1977.

[3] Orphal D.L., Borden W.F. Larson S. A. and Shultz P.H., Impoact melt generation and transport. *Proc. Lunar Planet. Sci. Conf. 11th*, 1980.

[4] Bjorkmann M.D and Holsapple K.A. Velocity scaling impact melt volume. *Int. J. Impact Engr.* 5, 155-163, 1987.

[5] Pierazzo E.,Vickery A.M., and Melosh H.J. A reevaluation of impact melt production. *Icarus* 127, 408-423, 1997.

EFFECTS OF TARGET PROPERTIES ON THE CRATERING PROCESS. K.R Housen, Shock Physics, MS 2T-50, The Boeing Co., P.O. Box 3999, Seattle WA 98124. kevin.r.housen@boeing.com.

Impact events in the solar system occur in a variety of materials, ranging from the rocky surfaces of the terrestrial planets to the icy mantles of the satellites of the outer planets to the undoubtedly highly fractured and porous materials that make up many asteroids and comets. A major challenge to impact modelers has been to understand how the composition and mechanical properties of these varied target materials dictate the outcome of an impact event. Four sources of information have historically been used to study this problem.

Scaling theory provides guidelines as to when specific material properties may have a significant effect on the outcome of an impact event. The initial work in scaling separated cratering events into the strength and gravity regimes. In the former, crater size is determined by the mechanical strength properties of the target while, in the latter, strength is unimportant compared to the effects of the lithostatic overburden. The transition between the two regimes is determined by the condition $Y/\rho gh$ = constant, where Y is a measure of target strength, ρ is the density, g is gravity and h is crater depth. This simplistic picture has now been modified in two ways. First, Gaffney and Holsapple [1] noted that the strength of many geological materials depends on the rate at which they are loaded and that loading rates depend on the size scale of the event. As a result, mechanical strength of the target decreases with increasing event size, so the transition into the gravity-dominated regime occurs at smaller crater sizes than the simple constant-strength model would predict. Second, numerical simulations by Nolan *et al.* [2] indicate that passage of the shock ahead of the expanding crater bowl pre-fractures rocky target materials, which allows the crater to form in an essentially cohesionless (but not strengthless) material. In essence, an impact event can alter the mechanical properties of the material in which the crater forms.

Scaling considerations have also been applied to impacts in highly porous targets [3, 4], which may be representative of comets and many asteroids. In this case, craters are formed mostly by compaction of pore spaces. Crater size is therefore determined by the crushing strength of the target. Impacts in these materials may not experience a gravity regime because at large size scales (where gravity would be expected to dominate), the material crushes to a point where the lithostatic compressive stress is comparable to the crushing strength. Hence, a situation is never attained in which gravitational stresses are large compared to the important strength measure.

In addition to mechanical strength, scaling analysis has been used to identify conditions under which target viscosity is the most important property in determining crater size. Cratering in a viscosity-dominated regime has been applied to studies of Martian rampart craters [5] and craters on icy satellites [6].

Scaling theory is essential to identify the conditions under which various target material properties might be important in determining crater size and morphology. However, scaling laws by themselves cannot establish the relation between crater size and material properties. Instead, experiments and code calculations must be used to determine those dependences.

Field explosion experiments are a second source of information on the effects of material properties. Field tests are especially useful in that they can be conducted at size scales much larger than laboratory experiments. The largest conventional explosion test conducted in the U.S. involved 4.36×10^9 g of explosive and produced a crater 88.4 m in diameter [7]. While still small by planetary standards, these craters are more than 100 times larger than those that can be studied in the lab. Additionally, field tests have been performed in various geologic settings and can be used to illustrate the dramatic effects of material properties. For example, Figure 1 compares the crater profiles produced in two tests involving hemispheres of high explosives with a mass of 4.5×10^8 g, one in basalt and one in unconsolidated alluvium.

Laboratory experiments have of course been the main source of information for cratering studies. An advantage of laboratory experiments is that they can be conducted under controlled conditions, whereas field tests are at the mercy of the natural settings under which they are conducted. That is, it would be difficult to determine the influence of material properties from field tests alone because a multitude of important properties may vary from one test site to the next. As an example, Figure 2 uses the results of impact experiments to addresses the dependence of crater size on target density. Cratering efficiency (target density * crater volume/impactor mass) is shown for three cohesionless granular materials whose bulk densities vary by a factor of 2.6. The results show that cratering efficiency in nearly independent of target density for this particular type of target material

A limitation of laboratory studies is that they are, by definition, conducted at small size scales. Therefore, if any important material properties are scale dependent (e.g. the strength of rock), then the experimental results will not be directly applicable to larger events and must consider the scaling issues involved with extrapolation to larger sizes.

Numerical simulations have become a popular method for studying crater formation and offer the potential benefit of being able to study the separate effects of material properties on crater size and morphology. While this benefit is alluring, a considerable drawback to code calculations is that the results are

only as good as the physical models that they incorporate. The constitutive models used in present codes such as CTH are reasonably accurate for some materials (e.g. metals), but are not well-developed for others, notably rock or highly porous soils. As a result, code results should be viewed with skepticism until validated extensively against laboratory and field tests [9]. Nevertheless, when such validations are accomplished, numerical simulations can provide tremendous insight into the effects of material properties.

Figure 3 presents an example. It was noted above that impact shock in rocky targets pre-fractures the material ahead of the expanding crater. This phenomenon has been used at times to assume that this pre-processing reduces the material strength to zero. While pre-fracturing should eliminate cohesion, the fractured rock will still have considerable strength in shear due to the effective friction angle associated with the interlocking of the rock fragments. The effect of friction angle is addressed in Figure 3, which shows the result of two CTH calculations of the Sailor Hat explosion event. Crater profiles are shown at an intermediate time during crater growth. The two simulations were identical except that the one on the left assumed a friction angle of 0° (equivalent to assuming a strengthless material), while that on the right shows a more realistic value of ~30°. These results show the significant effect that the material shear strength has on crater formation; an effect that is ignored in many calculations reported in the literature.

Additional calculations are underway. These results, along with those from scaling, field tests and laboratory experiments will be summarized to identify what is and is not known about the effects of material properties on crater formation.

References: [1] Gaffney E.S. and Holsapple K.A. (1983) Crater scaling relations for strain-rate dependent materials, (Unpublished report). [2] Nolan M.C. *et al.* (1996) *Icarus* 124, 359-371. [3] Housen K.R. *et al.* (1999) *Nature* 402, 155-157. [4] Housen K.R. and Holsapple K.A. (2002) Submitted to *Icarus*. [5] Gault D.E. and Greeley R. (1978) *Icarus* 34, 486-495. [6] Fink J. *et al.* (1984) *J. Geophys. Res.* 89, 417-423. [7] Lee C.K.B. and Mazzola T.A. *J. Geophys. Res.* 94, 17,595-17,605. [8] Holsapple K.A. and Housen K.R. (2002). *LPSC* Abstract.

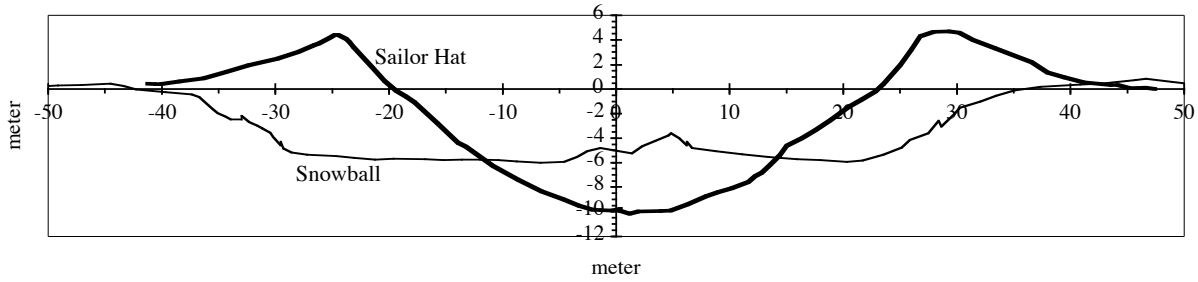

Figure 1. Comparison of crater profiles from two explosive field tests. Both tests used hemispherical charges of TNT (4.5×10^8 g) situated at the target surface. The Sailor Hat event was conducted in basalt, whereas Snowball was conducted in unconsolidated alluvium with the water table at a depth of approximately 7 m.

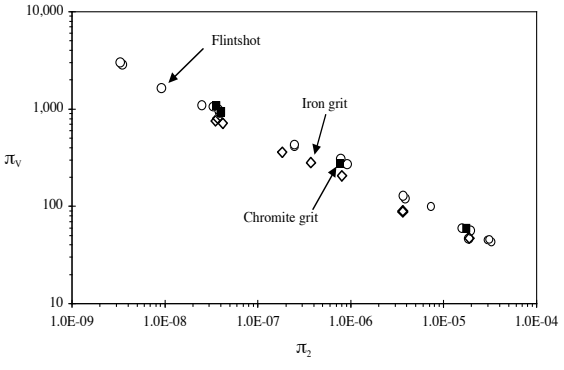

Figure 2. Cratering efficiency, π_V, vs π_2 for 1.8 km/s impacts into three granular cohesionless materials of density 1.8 (Flintshot sand), 3.1 (Chromite sand) and 4.6 gm/cm^3 (Iron sand). These data show that cratering efficiency is nearly independent of target density.

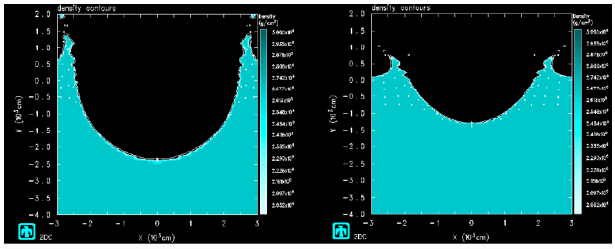

Figure 3. Comparison of two numerical simulations (CTH) of the formation of the Sailor hat explosion crater. The crater profiles are shown at an intermediate time of 0.18 s. Both models assume a Mohr-Coulomb behavior. The Profile on the left is for a case where the angle of internal friction is zero, while the case on the right is for approx. 30°. The formation time of the crater is ~0.5 s.

COMPLEX CRATER FORMATION: VERIFICATION OF NUMERICAL MODELS. B. A. Ivanov, Institute for Dynamics of Geospheres, Russian Academy of Sciences., Leninsky prospect., 38-6, Moscow, 117334, Russia (baivanov@onlime.ru, ivanov@lpl.arizona.edu).

Introduction: The growing capability of modern computers offers increased possibilities for numerical modeling of impact crater formation. However, complex crater formation include various particular models of rock massifs dynamical behavior in a wide range of thermodynamic parameters and strain rates. At the same time geological and geophysical investigations of impact craters give only the final structure of craters and geophysical fields around. The verification of numerical models should take into account comparison of computed results with maximum possible set of observational data.

Ground truth: The list of parameters one should compare includes crater morphology and morphometry, deformation of stratigraphic layers and their structural uplift; impact melt volume; shock wave decay; geometry and size of fractured zone, and individual specific features available for some terrestrial craters (presence of tektites, evidences of underwater formation etc.).

Primary experience: The list of recent publication gives an impression about strong and weak topics in the current state of model's verification.

Crater morphology and morphometry.. Models for many craters has been published, however rare papers deals with a systematic investigation of a crater shape in a wide range of crater diameters with the *same model*. A good example is done in [1] where the depth/diameter relation bend is reproduced qualitatively for the moon, Earth and Venus. However, quantitative fit of models to measurements is still an open question.

Deformation of stratigraphic layers and their structural uplift. First attempts to compare models for specific craters has been published for Chicxulub [2] and Puchezh-Katunki [3]. Again, qualitative fit of models is obtained with many quantitative misfits.

Impact melt volume is the best-studied model value [4] ready to be compared with observational data [5]. One can state the good fit of models to field data. The fit demonstrate that current scaling laws allow us to estimate impact energy for a given crater with the accuracy of factor of 2. However, the melt production in oblique impacts is still under investigation [6, 7].

Shock wave decay is easy to get in a numerical model and is very hard to compare with observations: due to a structural uplift formation the final position of shocked rocks are very far from their initial position in a target. Hence only full model of a complex crater modification allow us to verify models with a shock wave decay [3] (Fig. 1).

Geometry and size of fractured zone are just began to be used in model/nature comparisons. Rare papers for several craters has been published (eg. [8]). At the same time namely modeling of a fracture zone allow to compare code results with available gravity and seismic survey. This direction looks like a promising way for future modeling evolution.

Individual specific features for several terrestrial craters allow to verify a complex interaction with layered targets. One can refer for recent estimates of a tektite origin [9] and underwater crater modeling [10]. The modeling of individual specific features is also fast evolving approach to verify numerical models of impact cratering.

Conclusion: Numerical models of complex impact crater formation can be and should be verified by comparison with field geological and geophysical data.

References: [1] Wünnemann, K.. et al. (2002) *LPS XXXIII*, Abstract #1277.. [2] Collins, G. S. et al. (2002) *Icarus 157*, 24-33. [3] Ivanov, B. A. (2002) *LPS XXXIII*, Abstract #1286. [4] Pierazzo E. et. al. (1997) *Icarus 127* 408-423.. [5] Grieve R. A. F. and Cintala M. J. (1992) *Meteoritics 27*, 526–538. [6] Pierazzo E. and Melosh H. J. (2000) *Icarus 145*, 252-261.[7] Ivanov B.A. and Artemieva N. A. (2002) *GSA Spec Paper 356*, 619-630. [8] O'Keefe, J. D.and Ahrens, T. J.(1999) LPS XXX, Abstract #1304. [9] Artemieva N.A. (2002) In *Impact studies*, Springer Verlag, Berlin, pp. 257-276. [10] Ormö, J. et al. (2001) MAPS 36, Suppl. p.A154.

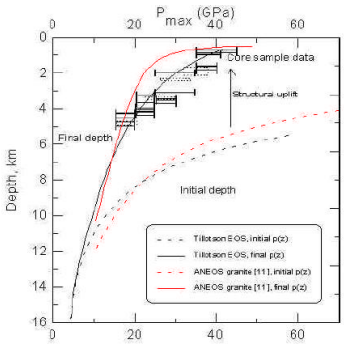

Fig. 1. The apparent shock wave decay with depth along the deep drill hole in the center of the Puchezh-Katunki crater, diameter D~40 km Maximum shock pressures recorded in minerals are shown as error bars. All EOS's used show that the central uplift top is constructed of rocks uplifted from ~6 km depth [3].

MODIFICATION OF ANEOS FOR ROCKS IN COMPRESSION. B. A. Ivanov, Institute for Dynamics of Geospheres, Russian Academy of Sciences., Leninsky prospect., 38-6, Moscow, 119334, Russia (baivanov@online.ru, ivanov@lpl.arizona.edu).

Introduction: The Analytical Equation of State (ANEOS) [1] is a useful computer code to generate equations of state (EOS) for rocks and minerals. An accurate EOS is one of essential points necessary for the numerical modeling of impact events. We analyze here a possibility to use a "standard" ANEOS in a "non-standard" way to make more flexible the procedure of an EOS construction.

ANEOS: The ANEOS Fortran package gives an opportunity to construct EOS for geomaterials, needed for the numerical modeling of planetary impact cratering. In comparison with the widely used Tillotson's EOS [2, 3], ANEOS has many advantages in respect to more accurate and self-consistent description of melting and vaporization. The practical convenience is that ANEOS gives the temperature of a material as an explicit output parameter. The calculation of temperature with the Tillotson EOS is possible (at least in compression) but needs an additional thorough treatment [4].

The original version of ANEOS [1] has several limitations which complicate its usage for rocks and minerals. The first one - monoatomic vaporization (good for metals and wrong for main minerals) - has been partially released by J. Melosh [5]. The second one - a simplified description of the solid-solid phase transition is the matter of the presented work.

Solid-solid phase transitions is a typical feature of shock (and static) compression for most of main rock-forming minerals (quartz, plagioclase, olivine etc.). ANEOS treats this phase transition via the modification of the "cold compression" curve. It is an elegant way to reproduce the complexity of the Hugoniot curve at a transition area. However, the simplicity of the approach has a high price: the thermal part of the EOS use the same parameters for the high pressure phase (hpp) and for low-pressure phase (lpp). For main rocks (granite, dunite) it leads to the artificially large heat expansion close to the normal pressure. Due to enlarged heat expansion an attempt to construct the Earth-like target with a typical geothermal gradient results in density decreasing with depth. for 10 to 100 km depth. Another disadvantage is that to use the solid-solid phase transition option one needs to switch out the melt curve construction.

HPP as a second material. We investigate here a possibility to "improve" ANEOS using it separately for hpp and lpp phase areas. A similar approach is used in the other "analytical" equation of state, PANDA [6, 7]. For each rock material we build the ANEOS input file as for 2 materials: hpp material and lpp material. The hpp material has a proper "shift" for energy and entropy to use the same reference level both for lpp and hpp. A relatively simple Fortran routine is added to compute the phase equilibrium between lpp and hpp. The parameter fit is conducted, as usual, via the comparison with available thermodynamic and Higoniot data for materials under investigation. The output for the following usage in hydrocodes is assumed to be in the form of tables.

Preliminary results. Currently we have tested two materials of interest - granite and olivine. For these rocks some experimental data on shock and released temperatures are available (eg. [8, 9]). Fig. 1 illustrates the output of the updated ANEOS for olivine showing the dependence of complete (*cm*) and incipient (*im*) meting pressure for the preheated target. The preliminary estimate for the *im* shock pressure of a pre-heated peridotite is shown for a comparison. Further testing would show is it a plausible way to "improve" ANEOS for rocks and minerals.

References: [1] Thompson, S. L., Lauson, H. S. (1972) *Sandia National Laboratory Report* SC-RR-71 0714. [2] Tillotson J. H. (1962) *Gen. At. GA-3216*, 140 pp. [3] Allen RT (1967) *Spec. Nuclear Eff. Lab. - Defense Atomic Support Agency:* DA49-146-XZ-462 16 p [4] Ivanov B. A. et al. (2002) *GSA Spec. Pap. 356*, 587-594. [5] Melosh H. J. (200) *LPS XXI*, Abstract # 1903. [6] Kerley G. I. (1989.) *High Pressure Res. 2*, 29–47. [7] Kerley, G. I. (1991) *Sandia Report SAND88-2291*, Albuquerque, NM,. 176 pp. [8] Holland K. G. and Ahrens T. J. (1997) *Science 275*, 1623-1625. [9] Lyzenga G. A. et al. (1983) *J. Geophys. Res*. 88, 2431-2444.

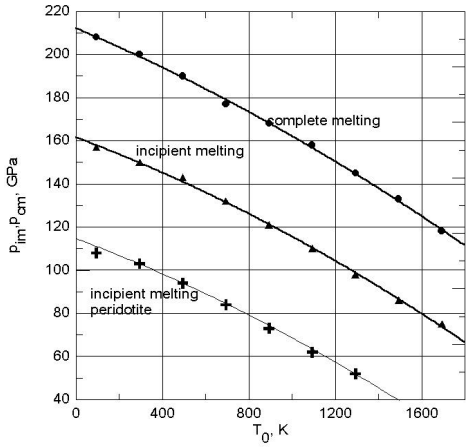

Fig. 1. Shock pressure for incipient and complete melting after a release for olivine and peridotite estimated with ANEOS.

EDUCATIONAL EXPERIENCE IN NUMERICAL MODELING OF IMPACT CRATERING. B. A. Ivanov, Institute for Dynamics of Geospheres, Russian Academy of Sciences., Leninsky prospect., 38-6, Moscow, 119334, Russia (baivanov@online.ru, ivanov@lpl.arizona.edu).

Introduction: The growing capability of the impact crater numerical modeling makes actual questions how to attract young students to the research and how to educate students specialized in general geology and geophysics. An experience in this direction has been accumulated in September 2002 during the ESF IMPACT Short Course "Numerical Modeling of Impact Crater Formation ".

Scope: The goal of the short course was to introduce basics of the numerical modeling techniques to non-professionals. "Non-professional" in this context means that the course was oriented to students and post-docs without a special background in computer science, shock wave physics and rock mechanics. However, most of students have an experience in impact crater related researches. Hence, all of them was highly motivated by their previous education and current research activity.

Attendance: 10 students from 6 European countries attended the short course (Germany - 3, France -2, Estonia - 2, Spain - 1, the Netherland -1, Finland -1). The general information about the ESF IMPACT program is available at http://www.esf.org WEB site.

Support and organization: The living and housing expenses have been covered by the ESF IMPACT program. The lecture room and the computer class have been offered by Vienna University (Prof. C. Koeberl was an excellent course manager). The computer class gives an opportunity for which student to work with a personal networked computer (PC under Windows 2000). The main lecturer (B. Ivanov) has used a beamer as for lecturing and for the demonstration of the practical work at the large screen. It was very important during the installation of the software and practice - students has seen simultaneously the output of each operation at their personal terminals and at the big ("master") screen repeated the "master" computer of the lecturer.

Short course program includes 5 main lectures and 5 practical lessons (totally 5 days with lectures before lunch and a practice in the computer class after lunch). Lecture topics include:

1. "What and how can be modeled for impact cratering. Shock waves, excavation and modification of a transient cavity".
2. "SALE hydrocode, general logic, input file, outputs"
3. "Equation of state (EOS). Ideal gas, Murnaghan, Mie-Gruneisen, ANEOS"
4. "Rock strength. Basics (elasticity, placticity, fragmentation/damage, dry friction). Implementation into hydrocodes. Acoustic fluidization"
5. "Examples of numerical modeling implementation in a geoscience research projects: Puchezh-Katunki deep drill core analysis, trigger volcanism, penetration of the Europa ice crust".

Practice includes software (Fortran compiler and a hydrocode) installation, the code compiling with a graphic package PGPLOT [1].

Numerical code used for the short course is based on the SALE code [2], enhanced with options to compute multimaterial problems (2 materials plus vacuum) in the Eulerian mode with a simplified description of rock's elastic-plastic behavior. The code with a working name "SALEB" is armored with 2 kinds of EOS's: Tillotson's EOS [3] with an addition for the real temperature estimates [4], and tabulated ANEOS [5] for several types of rocks.

Practice includes the solution of 3 problems: shock recovery container (calcite in the iron container), vertical crater-forming impact, oblique 2D (planar) impact. Students have been asked to compute several variants changing the input file parameters to get an impression about sensitivity of results. Naturally, only initial stages has been modeled during the class hours.

Handouts included a CD ROM with the source code and a set of publications relevant to the topic. In addition, each lecture, prepared in PowerPoint has been printed out as handouts.

Conclusion. The experience with the short course shows that it is possible to organize a "quick entry" to the topic in a relatively short time for highly motivated students. Post-course correspondence shows that at least 4 students continue to work with the code. It is early to say is the course enough to begin a real numerical research. However, one can hope that the course will help all students to understand better publications about numerical modeling.

References: [1] http://astro.caltech.edu/~tjp/pgplot/. [2] Amsden A. et al.. (1980). *Los Alamos National Laboratory Report LA-8095*, Los Alamos, NM, 101pp. [3] Tillotson J. H. (1962) *Gen. At. GA-3216*, 140 pp. [4] Ivanov B. A. et al. (2002) *GSA Spec. Pap. 356*, 587-594. [5] Thompson, S. L., Lauson, H. S. (1972) Sandia National Laboratory Report SC-RR-71 0714.

COOLING OF THE KÄRDLA IMPACT CRATER: II. IMPACT AND GEOTHERMAL MODELLING. A. Jõeleht[1], K. Kirsimäe[2], E. Versh[3], J. Plado[4] and B. Ivanov[5], [1,2,3,4]Institute of Geology, University of Tartu, Vanemuise 46, 51014 Tartu, Estonia; [1]ajoeleht@ut.ee, [2]arps@ut.ee, [3]desty@ut.ee, [4]jplado@ut.ee; [5]Institute for Dynamics of Geospheres, Russian Academy of Sciences, Leninsky Prospect 38-6, Moscow 117979, Russia, baivanov@idg.chph.ras.ru.

Introduction: Hydrothermal mineralization has occurred in many impact craters including also a 4-km marine complex crater in Kärdla, Estonia. Mineralogical and fluid inclusion data [1,2] provide temperature ranges for different mineralization events and, thus, giving a starting point for modelling. Modelling includes both (1) impact modelling to get the structure and temperature distribution in crater rocks right after the impact, and (2) geothermal modelling to get information on heat transfer processes and time-scale of post-impact cooling.

Impact Modelling: The target in Kärdla was about 150 m thick sedimentary layer on top of crystalline basement [3]. The impact took place in a ~100 m deep epicontinental Ordovician sea. SALE hydrocode was used to simulate formation, modification, and impact-induced heating in Kärdla crater. Both Tillotson equation of state and ANEOS algorithm were tested.

Modelling results suggest that usage of Tillotson equation of state gives very poor estimate of impact heating effect. It gives a temperature rise of ~100 K only, which contradicts with temperature of at least 300°C proven by PDF studies, quartz fluid inclusion homogenization temperatures, and chloritization geothermometry [1]. Maximum temperature estimate of 450°C [1] relies on formation of K-feldspar prior chloritization and maximum fluid inclusion homogenization temperature estimates. Results obtained using ANEOS algorithm are in better agreement with observations and suggest maximum temperatures of 300-350°C.

The crater is filled with resurge deposits which are at least 170 m thick. Unfortunately we were not able to simulate resurge flow and formation of resurge gullies with 2-D software in axisymmetric coordinates.

Geothermal Modelling: Post-modificational temperature distribution in crater rocks was one of the input parameters for transient fluid flow and heat transfer simulations for 2-D axisymmetric case. Fluid and rock properties were temperature-dependent. Effects due to fluid phase changes and associated latent heat effects were also implemented in the software.

The phase change of water has a double effect on heat transfer. First, when water vaporizes, its density decreases by more than one order of magnitude resulting in high buoyancy and rapid upward flow. Second, vaporization requires additional (latent) heat, which is absorbed from surrounding rocks resulting in their effective cooling at the high water vaporization rates.

The preliminary results suggest that vaporization of upward flowing fluid contributes significantly to cooling, decreasing the maximum temperature below boiling point (~ 250°C in case of Kärdla) in a few tens to hundreds of years. Heat transfer by liquid fluid is not as powerful as in vapor phase. The radiative heat transfer would start to contribute noticeably at temperatures above 600 °C, but is insignificant in Kärdla-size crater because of too low temperatures even immediately after the impact.

In the early stage of cooling, convective heat transfer prevails whereas at later stage conduction dominates. The ratio of convection over conduction (Peclet number) depends largely on assumed permeability structure. Direct measurements give information only about present day permeability, therefore, detailed investigations are needed to estimate the decrease of permeability due to closure of pores by hydrothermal mineralization.

It should be noted that the same hydrothermal mineral precipitated at a different time at different location inside the structure. Because different parts of the crater cooled at different rate the lifetime of hydrothermal mineralization varied. For example, at comparable depths the rocks in central uplift are not cooling as fast as rocks near the ring depression because, in respect to groundwater convective system, they are located at discharge and recharge areas, respectively. Rocks at rim might have got additional heat by upward flowing fluid.

Cooling to ambient temperatures in the central part of the crater lasts for thousands of years. Despite of relatively rapid cooling, the thermal perturbations in the deeper part of the central uplift should be observable with geothermal tools even a few tens of thousands of years after the impact.

References: [1] Versh et al (2003) in this volume. [2] Kirsimäe et al. (2002) *Meteoritics & Planet. Sci., 37*, 449–457. [3] Puura & Suuroja (1992) *Tectonophysics*, 216, 143-156.

SEISMIC INVESTIGATION AND NUMERICAL MODELING OF THE LAKE BOSUMTWI IMPACT CRATER. T. Karp[1], N. A. Artemieva[2] and B. Milkereit[3], [1]Institute for Geosciences, Dept. of Geophysics, Kiel University, Otto-Hahn-Platz 1, 24118 Kiel, Germany, tkarp@geophysik.uni-kiel.de; [2]Institute for Dynamics of Geospheres, Leninsky pr., 38, bldg.6, 119334, Moscow, Russia, nata_art@mta-net.ru; [3]Dept. of Physics, University of Toronto, 60 St. George Street, Toronto, Ontario M5S1A7, Canada, bernd@core.physics.utoronto.ca

Introduction: The Lake Bosumtwi impact crater, Ghana, (age 1.07 Ma, diameter 10.5 km) is one of the youngest and best-preserved complex terrestrial impact structures. It was excavated from hard crystalline target rock and is the source of the Ivory Coast tektite strewn field. It is almost entirely filled by the Lake Bosumtwi.

Seismic investigations of the Bosumtwi crater identify the proposed central uplift [1] and indicate a low-velocity breccia-layer below the lake and the post-impact sediments [2]. Recent evaluation of a longer seismic refraction line extends information on velocity-depth distribution down to ~1.7 km (Fig. 1). The structure is characterized by a vertical velocity gradient. Lateral velocity variations also occur. Higher seismic velocities are observed right below the central uplift, north and south of it velocities are lower. The area of higher velocity is interpreted to consist of uplifted basement originally situated at greater depth. The area of lower velocity is interpreted to be an allochthonous breccia cover surrounding the uplift. A distinct interface between the breccia layer and brecciated crater floor cannot be resolved. Lateral velocity changes occur down to a depth of 1.6 km below the lake indicating that rocks are brecciated down to at least this depth. The structural uplift is estimated by the 3.9 km/s-isoline to be at least 800 m. The apparent depth of the crater is 550 m.

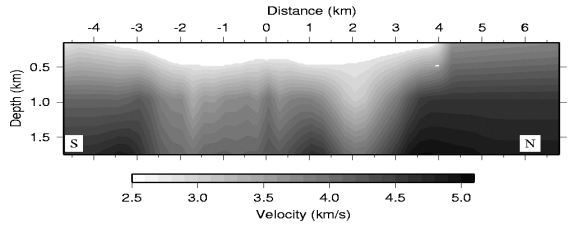

Fig. 1: Seismic velocity distribution of the Bosumtwi crater. Vertical reference is the estimated original target surface (150 m above lake surface). White area corresponds to water and post-impact sediments.

Numerical modeling of the crater is performed (1) with the SALE code to receive final crater shape after a vertical impact, and (2) with the SOVA code to model an oblique impact and tektites production. Projectile size estimates with scaling laws [3] vary in the range 400 - 1600 m, depending on impact angle and velocity. ANEOS equation of state for granite is used to describe both the target and the projectile.

Vertical impact and final crater shape. To simulate the temporal decrease of friction in rocks around a growing crater the "block model" (a version of the general acoustic fluidization model) is used [4]. Projectile velocity is 12 km/s, diameter is 750 m. The "block model" parameters for Bosumtwi have been published in [5]. The modeled rock mechanics include the gradual shear failure, an instant tension failure, the decrease of strength and internal friction close to the melt temperature, and the pressure dependence on the melt temperature. Variations of friction for damaged materials (0.2 - 0.5) and decay time for block oscillations (9 - 15 s) will produce a ~10 km in diameter crater, 200-300 m deeper than seismic data reconstruction (Fig. 2). Reasons for this discrepancy may be: (1) dilatancy of damaged rocks (not yet included); (2) deposition of fallout ejecta (suevite) inside the crater (in 2D models the ejected material is deposited outside the crater); (3) an oblique impact produces a shallower crater, but no strength model for 3D modeling is currently available.

Oblique impact and tektites. Most suitable conditions for tektite origin arise in the case of high-velocity impact (>20 km/s) with impact angle 30°-50°. 3D modeling shows that the fallout ejecta thickness inside the crater does not exceed 30-40 m. This is too thin to fill the gap between modeled and observed profiles.

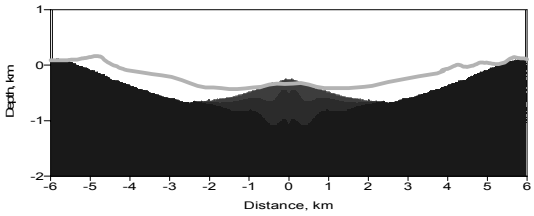

Fig.2: Density distribution after 100 s represents final crater shape obtained with the SALE modeling. Seismic-topographic profile is shown as grey line.

Discussion: Numerical modeling allows partial reconstruction (diameter, central uplift) of the Bosumtwi crater. Dilatancy and obliquity have to be included. Results from gravity and magnetic surveys and future scientific drilling (ICDP) will refine structural information of the crater and improve modeling results.

Acknowledgements. This work was financially supported by DFG grant Ja 290/15-2. We thank Boris Ivanov for the help with the SALE-modeling and useful discussions.

References: [1] Scholz et al. (2002) *Geology 30 (10)*, 939-942. [2] Karp et al. (2002) *Planetary and Space Science 50 (7-8),* 735-743. [3] Schmidt R.M. and Housen K.R. (1987) *Int. J. Impact Engn 5,* 543-560. [4] Melosh H.J. and Ivanov B. (1999) *Ann. Rev. Earth and Plan. Sci. 27*, 385-415. [5] Ivanov B. and Artemieva N. (2002). *GSA Spec. Paper 356*, 619-630.

EARLY FRACTURING AND IMPACT RESIDUE EMPLACEMENT: CAN MODELING HELP TO PREDICT THEIR LOCATION IN MAJOR CRATERS? A. T. Kearsley[1], G. A. Graham[2], J. A. M. McDonnell[3], P. A. Bland[4], R. M. Hough[5] and P. A. Helps[6]. [1] Space Science Research, BMS, Oxford Brookes University, Oxford, OX3 0BP, UK, ***atkearsley@brookes.ac.uk***; [2] IGPP, LLNL, Livermore, California, USA; [3] Planetary and Space Sciences Research Institute, The Open University, Walton Hall, Milton Keynes, MK7 6AA, UK; [4] Department of Earth Science and Engineering, Exhibition Road, Imperial College of London, South Kensington Campus, London SW7 2AZ, UK; [5] Museum of Western Australia, Francis St, Perth, WA 6000, Australia; [6] School of Earth Sciences and Geography,Kingston University, Kingston-upon-Thames, Surrey, KT1 2EE, UK.

Introduction: In a field investigation of a crater, where are the most effective places to look for material that could reveal the nature of object responsible for the impact? Can numerical modeling of impact processes help to predict locations in which recognisable residue of the bolide could be found?

Locations of Residue Preservation: The nature of an extraterrestrial body whose hypervelocity impact has created a terrestrial impact crater can sometimes be determined by collection of disrupted and shocked impactor fragments as loose fragments or within small bodies of impact melt from the ground surface in and around the crater: e.g. iron meteorites from the vicinity of Barringer Crater, (USA); Henbury (Australia); Sikhote Alin (Siberia), meteoritic debris and impact glasses from Lonar (India), Wabar (Saudi Arabia) and Monturaqui (Chile); and even meteoritic debris from the Eltanin impact (SE Pacific), sampled from the deep sea [1]. If a major melt component is still preserved at the crater e.g. glass bombs within the suevites at Ries (Germany) or as a substantial discrete melt body as at Popigai (Siberia), materials suitable for bulk trace-element or isotopic analysis may also be relatively easy to collect. When an impact feature has been substantially modified by subsequent erosion (e.g. Sierra Madera, Texas), it may prove more difficult, or impossible, to find chemical residue from the bolide for analysis. Characteristic large-scale impact-related structures, (e.g. central uplifts and ring-synclinoria) may remain, with diagnostic shock indicators (e.g. shatter cones, planar deformation features and high pressure mineral polymorphs), yet the ejecta-blanket and any impact melt body are lost.

Residues and Fractures: Some eroded structures do retain extraterrestrial residues and debris derived from higher structural levels, emplaced within fractures, e.g. 'Granophyre Dykes' into granulite facies basement at Vredefort (R. of South Africa) [2], and breccias in rim rocks at Roter Kamm (Namibia) [3]. For residue to penetrate along these fissures, is it not likely that fracturing must occur very early in the crater-forming process? In some craters there is also substantial outward motion of target debris along major radial fractures, such as the 'Offset Dykes' at Sudbury [4]. Outward compressive motion has been seen in the reverse faults of the Chicxulub [5] and Silverpit [6] craters, also implying an early origin for these planes of movement. How often are major fractures created during early phases of crater growth? How widespread is residue emplacement into fractures?

Metallic residues, in melts and fractures: Distinctive, fine-scale siderophile segregations occur at a number of smaller (km scale) craters. At Lonar, Wabar, Monturaqui and Barringer, metallic residue is intimately associated with impact products, within silicate glass, vesicles, and brecciated rock fragments, or as thin coatings on target rock clasts. Residual metal may have a typical meteoritic Fe:Ni ratio, but often shows substantial modification of composition during and after impact. In a single small impactite specimen there may be metallic grains of widely differing texture and composition, with local enrichment of nickel and cobalt, and loss of iron to silicate-rich melt (Figure 1).

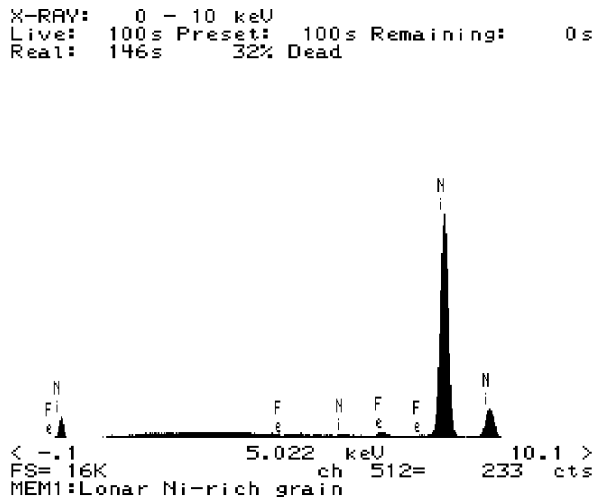

Fig. 1. Energy dispersive X-ray spectrum of Nickel grain from Lonar impactite.

Where iron-bearing oxides, such as ilmenite, occur in the target rocks, as in the basalts of the Lonar crater, metal may also be generated by mineral dissociation. The characteristic titanium content and the close proximity of melt droplets to remnant titanium oxides distinguish this metal from true impactor residue.

At the Ries crater, brecciated and foliated granitic igneous basement rocks, cored in the Nördlingen 1973 borehole, contain dispersed tiny nickel grains, perhaps similar to [7], and whose abundance can reach levels equivalent to 660 ppm in the whole rock. Occurrence of these distinctive grains implies that modified impactor components were emplaced into deep target rock, subsequently uplifted during crater modification.

Evidence from small impact craters: As part of a separate study [8], we have made an extensive survey of millimeter-scale impact craters on brittle, laminated glass solar cells exposed to hypervelocity collision (typical velocity 25 km s^{-1}) during exposure in low Earth orbit on the Hubble Space Telescope. Craters may contain particulate impactor residue in fractures, as well as in a thin melt sheet. The fractures have previously been considered late-stage features, and due to extensional failure (spallation) close to the glass surface, following passage of a shock wave through the laminate structure. However, the presence of included micrometeoroid fragments suggests that the fractures must be formed early. Our laboratory experiments, utilising a range of mineral and metal grain projectiles accelerated to c. 5 km s^{-1} in a light gas gun (LGG), have revealed that delicate, volatile-rich residues can be emplaced into fractures around small craters on a variety of brittle substrates such as glasses and rocks.

Numerical modeling of crater formation: Modeling of small impacts [9], using AUTODYN 2D, has revealed that fractures can be generated at a surprisingly early stage in the impact process, prior to rebound of the crater floor and ejection of the bulk of remnants of the impacting body (Figure 2).

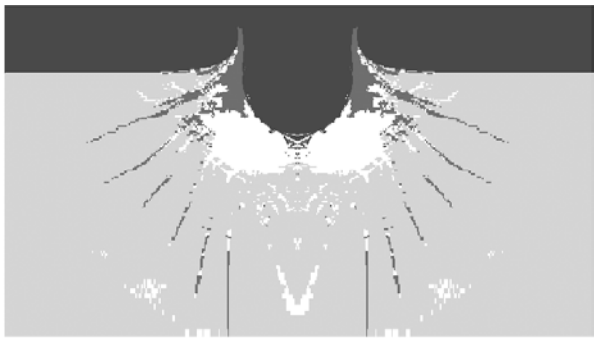

Fig. 2. AUTODYN 2D simulation of hypervelocity impact of a small metal sphere onto a glass target. Dark grey areas indicate failure, including fractures.

The model fractures correspond in position and orientation to locations in which we have observed residue in both space-exposed craters and laboratory light gas gun impacts. Numerous authors have shown that numerical modeling can be remarkably successful in simulation of larger features of crater development, and can account for many structures recognized during field examination of larger terrestrial craters. The significance of small (metre-scale) brittle structures in and around terrestrial impact craters is also becoming apparent from both modeling and field studies [10]. Important questions that have not yet been fully addressed include the timing and location of major fracture development in relation to the availability and possible pathways of bolide residue material. Tracing 'tagged' projectile material throughout the duration of the modeling process might prove rewarding. The potential role of early-formed fractures in outward transport, thickening of the pre-impact stratigraphic sequence, and localisation of structural weaknesses that permit subsequent inward crater collapse may also prove worthy of further investigation.

Conclusions: We believe that distinctive nickel-enriched residues can be used to track the presence of processed meteoritic metal. Small grains and melt droplets can be emplaced within silicate impact melts, within vesicles and within fractures in both impact clasts and deeper into basement. These observations imply that the fractures must have been present at a stage when bolide remnants were still abundant. Evidence from both space-exposed and laboratory-simulated hypervelocity impacts of small projectiles suggests that small craters can develop extensive fracturing at an early stage, when impactor residue is still available to be emplaced. Although we do not suggest that the results of simulation from a mm-size should be scaled to km-size craters, our intriguing results suggest that modeling the early brittle responses of geological materials in larger, lithified, stratified target sequences may help to explain the distribution of fracturing and residue emplacement in and around major craters. Such models may help to constrain the optimum sites for sampling around eroded craters.

Acknowledgements: Jon Wells (Oxford Brookes University) for preparation of polished sections, Gerhard Drolshagen (ESA/ESTEC) for the use of Hubble Space Telescope solar cells and Mark Burchell (The University of Kent) for some of the LGG shots.

References: [1] Kyte F. (2002) pers. comm. [2] Koeberl C. et al. (1996) *Geology*, *24*, 913-916. [3] Degenhardt J. J. et al. (1994) *GSA Special Paper 293,* 197-208. [4] Spray J. G. (2001) pers. comm. [5] Morgan J. and Warner M. (1999) *Nature*, *390,* 472-476. [6] Stewart S. A. and Allen P. J. (2002) *Nature*, *418*, 520-523. [7] El Goresy A. and Chao E. C. T. (1976) *EPSL, 31*, 330-340. [8] Graham G. A. et al. (2000) *Adv. Space Research, 25*, 303-307. [9] McDonnell J. A. M. et al. (2001) *Int. Jour. Imp. Eng. 26,* (1-10), 487-496. [10] Kenkmann T. and Ivanov B. A. (1999) *LPS XXX*, Abstract #1544.

CRATER BASIN REBOUND ABOVE PLASTIC LAYERS: MODEL BASED ON EUROPA. Akos Kereszturi (Department of Physical and Historical Geology, Eötvös Loránd University of Sciences, H-1083 Budapest, Ludovika tér 2., Hungary, E-mail: krub@freemail.hu)

Introduction: Isostatic rebound and megaslumpings are important processes in the modification of large craters. Beside the exmaples for these on Mercury, Moon, Earth, Callisto (possibly Venus and Mars) we have good images from Europa. Analysis of internal rings and benches of great (usually greater than 100 km) craters and palimpsests help in the reconstruction of formation. The its young, pristine and tectonically homogene surfaced Europa can improve our knowledge in the reconstruction of crater basin formation.

The modell: Based on our up to date knowledge, the origin of the circular – and not central – ring structures are the follows (Fig. 1.) [1]: 1. Outcrops of isostatically uplifted internally layered matter [2],

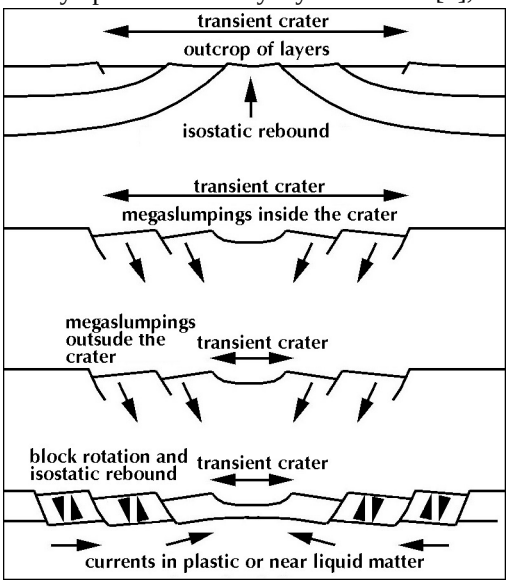

Fig. 1. Possible theories for the origin

2. Mega-slumpings inside the crater. 3. Megaslumpings outside the crater. 4. Block rotation and isostatic lifting [3]. With the analysis of the great craters of Europa we can nearly rule out the internal layering and slumping theories in the formation. Because of the thin ice crust Europa can serve as a unique modell for the crater formation on terrains with small lithospheric thickness, and it gives the possibility for the analysis of ancient craters on the Earth and current craters on Venus with relative thin litospheres.

Results: We analysed 32 relative great craters on icy moons, the best examples of them are on Europa (Fig. 2.). We make a somewhat similar analysis for the greatest basins on rocky bodies (eg. Caloris, Orientale, Argyre). We measured the diameters of the structures, the topography, the distribution of certain structures according to the crater diameter/the possible thickness of the lithosphere/cryosphere, distance from the center. The greatest problem is the definition of the original crater rim or the transient crater and to devide the internal rings from the outer narrow tectonic structures. We suggests: 1. Structures are originated by isostatic re- bound and not by megaslumpings or outcrops of layered matter. 2. Circular faults ouside the original craters form in great number on icy bodies. In the future we will extend the analysis: 1. Relation between possible transient crater diameter and outer rings. 2. To make „evolutionary sequence" for giant craters with rebounded floors accourding to the reaction of the lithosphere and gravity [5,6], which can be useful in the analysis of ancient rheologic conditions in rocky bodies.

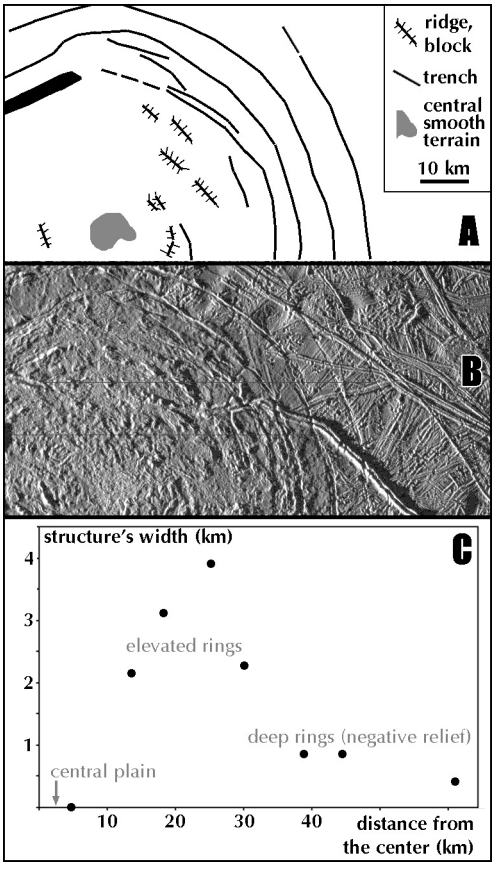

Fig. 2. Example structures

References: [1] Dence, M.R. et al. (1977) Terrestrial impact structures, Perrgamon Press, 1977. [2] Milton, D.J. et al. (1972) Displacement with impact craters, Proc. 24th Int. Geol. Congr. [3] Roddy, D.J. (1977), Large-scale impact and explosion craters, Pergamon Press, 1977. [5] Melosh H.J. (1989) Impact Cratering, Oxford Univ. Press. [6] Baldwin R.B. (1981) in Multiring Basins, LPI.

USING GEOCHEMICAL OBSERVATIONS TO CONSTRAIN PROJECTILE TYPES IN IMPACT CRATERING. Christian Koeberl, Institute of Geochemistry, University of Vienna, Althanstrasse 14, A-1090 Vienna, Austria (e-mail: christian.koeberl@univie.ac.at).

Introduction: Breccias and melt rocks found at possible meteorite impact structures on Earth may contain a minor extraterrestrial component. In the absence of evidence of shock metamorphic effects in such rocks, the unambiguous detection of an extraterrestrial component can be of diagnostic value regarding the impact origin of a geological structure. The verification of an extraterrestrial component in impact-derived melt rocks or breccias can be of diagnostic value to provide confirming evidence for an impact origin of a geological structure. Similar approaches are of great value in the investigation of distal ejecta layers (as we are taught by the case history of the Cretaceous-Tertiary boundary).

Qualitatively speaking, a small amount of the finely dispersed meteoritic melt or vapor is mixed during the impact event with a much larger quantity of target rock vapor and melt, and this mixture later forms impact melt rocks, melt breccias, or impact glass. In most cases, the contribution of meteoritic matter to these impactite lithologies is very small (<<1%), leading to only slight chemical changes in the resulting impactites. Geochemical methods can be used to determine the amount of such a meteoritic component (see below). However, there are plenty of open questions.

Methods: The detection of such small amounts of meteoritic matter within the normal upper crustal compositional signature of the target rocks is rather difficult. Only elements that have high abundances in meteorites, but low abundances in terrestrial crustal rocks (e.g., the siderophile elements) are useful. Another complication is the existence of a variety of meteorite groups and types, with widely varying siderophile element compositions. Distinctly higher siderophile element contents in impact melts, compared to target rock abundances, can be indicative of the presence of either a chondritic or an iron meteoritic component. Achondritic projectiles (stony meteorites that underwent magmatic differentiation) are much more difficult to discern, because they have significantly lower abundances of the key siderophile elements. Furthermore, in order to reliably constrain the target rock contribution of such elements, i.e., the so-called indigenous component, absolute certainty must be attained that all contributing terrestrial target rocks have been identified and their relative contributions to the melt mixture are reasonably well known.

Geochemical methods have been used to determine the presence of the traces of such an extraterrestrial component (see review [1]). Meteoritic components have been identified for just over 40 impact structures [1], out of the more than 160 impact structures that have so far been identified on Earth. The identification of a meteoritic component can be achieved by determining the concentrations and interelement ratios of siderophile elements, especially the platinum group elements (PGEs), which are several orders of magnitude more abundant in meteorites than in terrestrial upper crustal rocks. Iridium is most often determined as a proxy for all PGEs, because it can be measured with the best detection limit of all PGEs by neutron activation analysis (which was, for a long time, the only more or less routine method for Ir measurements at sub-ppb abundance levels in small samples).

The use of PGE abundances and ratios avoids some of the ambiguities that result if only moderately siderophile elements (e.g., Cr, Co, Ni) are used in an identification attempt. However, problems may arise if the target rocks have high abundances of siderophile elements or if the siderophile element concentrations in the impactites are very low. In such cases, the Os and Cr isotopic systems can be used to establish the presence of a meteoritic component in a number of impact melt rocks and breccias (e.g., [2]). In the past, PGE data were used to estimate the type or class of meteorite for the impactor, but these attempts were not always successful. It is difficult to distinguish among different chondrite types based on siderophile element (or even PGE) abundances, which has led to conflicting conclusions regarding the nature of the impactor at a number of structures (see [1]). Clearly, the identification of a meteoritic component in impactites is not a trivial problem.

Open Questions: Apart from analytical challenges, there is a whole suite of problems or questions associated with the identification of projectiles, which will be listed here in no particular order.

Some meteorite types do not have chemical compositions that are well enough separated from terrestrial rocks to allow a geochemical distinction in melt rocks. The chemical composition of specimens of the same meteorite type is not uniform, but shows a range of compositions. In addition, only a few samples of each type have been analyzed with enough detail to allow use of the data for mixing calculations. It is not yet possible to distinguish between comet and asteroid sources due to the lack of trace element data on a sufficient number of comet nuclei samples.

More peculiar, and possibly a point in which modeling calculations can be of use, is the very strange discrepancy between the interelement ratios of siderophile elements in impact glasses found at small impact craters and equivalent ratios in corresponding meteorite fragments found at the same craters (e.g., Meteor Crater, Wolfe Creek, Henbury, Wabar). No immediate physical explanation, or correlation with chemical and physical parameters, which could explain this fractionation, is available. In some other cases (e.g., Tswaing-Saltpan, Bosumtwi) there is a good fit for, e.g., Cr, Co, and Ni ratios and abundances between a particular meteorite type (e.g., chondrite), but the Ir abundances are about a factor of 2-10 too low for a chondritic projectile (which might otherwise also be confirmed by isotopic data). Why are some of the more refractory siderophile elements depleted? Is there some non-equilibrium process going on in the impact vapor plume?

Another interesting item are tektites. Tektites are natural glasses occurring on earth in four distinct strewn fields: Australasian, Ivory Coast, Central European, and North American. Ages of these strewn fields range from 0.78 to 35 million years. Geochemical arguments have shown that tektites have been derived by hypervelocity impact melting from terrestrial upper crustal rocks. Tektites are distal ejecta, which do not occur directly at a source crater, in contrast to impact glasses, which are found directly in or at the respective source crater. This has made the identification of the source crater somewhat difficult. Nevertheless, at least two of the four Cenozoic tektite strewn fields have been associated with known impact craters: the Ries crater in southern Germany and the Central European field, and the Bosumtwi crater in Ghana and the Ivory Coast field are rather firmly linked. In addition, the 85 km diameter Chesapeake Bay impact structure is a likely source crater for the North American tektites. This leaves the Australasian tektites as the only strewn field without a clear choice for a source crater.

Not much is known about the source meteorites (projectiles, meteorite types) for the four tektite fields. Attempts to determine of a meteoritic component in Australasian tektites has not yielded unambiguous results. Some Ni-Fe-rich spherules in philippinites, which were suggested to be a remnant of meteoritic matter, were later concluded to have formed by in-situ reduction from target material. Analyses of australites by radiochemical neutron activation analysis for a selection of volatile and siderophile element concentrations was not very conclusive either - only one of these samples showed a distinct enrichment in siderophile elements, while the other five do not indicate such an enrichment. On the other hand, Ir enrichments were found in several microtektite-bearing deep-sea sediment layers.

Regarding the Ivory Coast tektites, some researchers suggested an iron meteorite projectile (based on chemical data), others (more recently suggested a chondritic projectile). Os isotopic data clearly showed the presence of a meteoritic component in the tektites. Unfortunately, the Bosumtwi crater is in an area of known gold mineralization, which lead to high and irregular siderophile element contents in the target rocks.

Not much information is available regarding the Central European tektites, where an achondrite has been proposed for the Ries crater bolide. No information at all is available regarding the Chesapeake Bay crater/North American tektites. Thus, the question of projectile identification for tektites is still an open one.

In general, tektites are very poor in meteoritic matter, which led to the suggestion that they cannot form by jetting, as products formed by jetting should have high meteoritic components. On the other hand, tektites clearly formed from the rocks closest to the terrestrial surface – in some cases there is a soil component discernable. However, some recent data show that high-Mg microtektites do seem to have a significant (a few percent) meteoritic component. It seems that natural observations are still able to provide some puzzling constraints for future modeling calculations.

References: [1] Koeberl C. (1998) in: Meteorites: Flux with Time and Impact Effects, eds. M.M. Grady et al., Geological Society of London Special Publ. 140, pp. 133-152. [2] Koeberl C. et al. (2002) in: Geological Society of America Special Paper 356, pp. 607-617.

AMELIA CREEK, NORTHERN TERRITORY, AUSTRALIA: A 20 × 12 KM OBLIQUE IMPACT STRUCTURE WITH NO CENTRAL UPLIFT. F. A. Macdonald[1] and K. Mitchell[2], [1]Division of Geological and Planetary Sciences, Mail Code 170-25, California Institute of Technology, Pasadena, CA 91125, USA, francis@gps.caltech.edu, [2]Gerringong, NSW, Australia.

Introduction: The Amelia Creek Structure is located in the Davenport Ranges of the Northern Territory, Australia at lat. 20˚55'S, long. 134˚50E. Shock metamorphic features are developed on the southern, down-range side of the structure. No central uplift is developed and the dimensions of the impact structure are at least 20 × 12 km.

Geological Observations: Geologically, the Amelia Creek structure is situated within the Proterozoic sedimentary and volcanic rocks of the southern Tennant Creek Inlier. The structure is characterized by a central syncline flanked by a series of ramping, SSW trending thrust sheets. The canoe-shaped central trough (syncline) runs NNE-SSW and is ~1 km wide and 5 km long. Shatter cones, impact breccias and hydrothermal deposits were also discovered during detailed mapping of the central region in June of 2002.

Shatter cones at Amelia Creek are prolific in many quartzite beds on the southern side of the structure (fig. 1), and are invariably oriented upward, which in itself excludes the possibility that the impact occurred before the regional folding at ~1700 Ma [1]. The surface distribution of shatter cones forms a crescent-like shape approximately 1 × 3 kilometers on the southern side of the structure, extending at least 4 km south from the central syncline. Similiar lithogies are present throughout the structure; however, shatter-cones are only developed on the southern, down-range side. Allogenic breccias are developed along many of the major thrust faults within the structure and show evidence of baked margins and shocked clasts.

Discussion: Most impacts occur obliquely, not vertically as typically modeled [3]. In very oblique impacts, the initial transfer of energy into the target is less efficient and the resulting craters are smaller for a given impactor mass and velocity [2]; oblique impacts should produce much shallower deformation than their more vertical counterparts, and perhaps central uplifts do not develop even for large structures.

Structurally, the level of erosion at Amelia Creek appears to be less than a kilometer, however, the exhumed land surface that makes up the flat tops of the hills across the Davenport Ranges is early Cambrian or late Neoproterozoic in age [4], indicating that the structure may have been buried for much of the Phanerozoic. Some breccias in and around the structure were originally mapped as Cambrian and Tertiary breccias [1], but they may actually be impact breccias and impact ejecta. Thus, the age of the structure remains equivocal until relationships mapped in earlier work [1] are verified.

The rocks up-range of the structure also appear to be anomalously deformed, so there is a distinct possibility that Amelia Creek is part of a crater field or a ricochet structure. On geological maps, Aster and aeromagnetic images, the total area of anomalous deformation around Amelia Creek is strikingly similar in shape to the extremely oblique impact structures on Mars and the Moon [3].

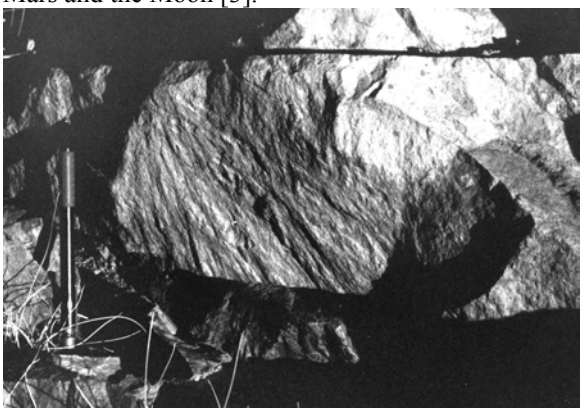

Fig. 1 Shatter cones on southern side of structure.

Conclusion: We believe that the shock metamorphosed rocks at Amelia Creek are the relict of an extremely oblique impact event. Evidence for this includes the elongation of the deformed area, the SSW direction of movement of most of the structural elements, the presence of a central trough and syncline in place of a central uplift, and the distribution of shatter cones only on the downrange side of the structure.

The mechanics of large, very oblique impact cratering is poorly understood [2]. This is due in part to the fact that no exposed, extremely oblique terrestrial impact structures have been previously reported [5]. As such, there are very few field measurements to put constraints on theoretical models. The impact-deformed rocks in the Davenport Ranges are incredibly well exposed, and this structure promises to be the world's type locality for oblique impacting.

References:

[1] Stewart A. J. et al. (1984), Expl. Notes of the 1: 250,000 Bonney Well Sheet, BMR.
[2] Melosh H. J. (1989) Impact Cratering: A Geologic Process. Oxford, 11.
[3] Schultz P.H., Gault D.D. (1990), GSA Sp. P. 247.
[4] Stewart A.J., et al (1986). Science 233, 758-761.
[5] Spray J.G. (2002) Earth Impact Database http://www.unb.ca/passc/ImpactDatabase/CINameSort.html

GOLDILOCKS AND THE THREE COMPLEX CRATER SCALING LAWS. William B. McKinnon,[1] Paul M. Schenk[2], and Jeffrey M. Moore[3], [1]Dept. of Earth and Planetary Sciences and McDonnell Center for the Space Sciences, Washington University, Saint Louis, MO 63130, mckinnon@levee.wustl.edu; [2]Lunar and Planetary Institute, 3600 Bay Area Blvd, Houston, TX 77058, schenk@lpi.usra.edu, [3]NASA Ames Research Center, Moffett Field, CA 94035, jmoore@mail.arc.nasa.gov.

Introduction: Formed in the gravity regime, complex craters are larger than their simple crater equivalents, due to a combination of slumping and uplift. Just how much larger is a matter of great interest for, for example, age dating studies. We examine three empirical scaling laws for complex crater size [1-3], examining their strengths and weaknesses, as well as asking how well they accord with previously published and new data from lunar, terrestrial, and venusian craters.

Croft (1985): The most widely quoted complex crater scaling is due to the detailed study of S.K. Croft [1]. He gauged the upper and lower limits to the position of the transient crater rim provided, respectively, by the terrace sets and central peak complexes of lunar and terrestrial complex craters. Added to these were a range of crater enlargements based on theoretical and experimental evidence for the geometric similarity of ejecta blankets [4]. Finally, a geometric restoration model was used to get an independent estimate. Bracketed mainly by terrace sets for craters closer to the simple-to-complex transition and central peak complexes of very large lunar craters (a size range that could have included peak-ring basins), he determined that the transient diameter D_{tr} scaled as $D^{0.85 \pm 0.04}$, where D is the final diameter. Inverting, we get

$$D = D_c^{-0.18 \pm 0.05} D_{tr}^{1.18 \pm 0.06} , \quad (1)$$

where D_c is the diameter of the simple-to-complex transition. A little remarked on aspect of this scaling law is that it nearly restores the diameter (through not the volume) of complex craters to strength scaling (i.e., D is proportional to $a^{0.92}$, where a is the impactor radius).

McKinnon and Schenk (1985): We used a transient crater restoration model for the Moon, based on Pike's lunar crater morphometric data [5]. Crater rims were restored using a range of constant slope angles for the ejecta deposit, with the restoration criterion being that the transient apparent (ground-plane) crater had a depth/diameter of $1/2\sqrt{2}$ [6]. Remarkably, the derived depth/diameter ratios for the full transient crater were close to constant, which is self-consistent support for transient crater geometric similarity. In terms of fit to a power law, we found

$$D = k D_{tr}^{1.13} , \quad (2)$$

where k is a constant. For the Moon, our k implied that simple craters near the simple-to-complex transition (~11 km from depth/diameter statistics) are ~15-20% wider than their original transient craters. This amount agrees with the amount of widening calculated for Brent and Meteor Craters due to breccia lens formation [6]. At the time it was less appreciated that all simple craters in rock are probably shallowed and widened by breccia lens formation. Breccia lens formation is something that has not been observed in laboratory impact studies to our knowledge (certainly not in dry sand), so direct application of sand crater scaling laws, even to simple craters, should be done with caution.

As for eq. (2), it can be put in the same functional form as eq. (1) if k is proportional to $D_c^{-0.13}$, and we recommend $k = 1.17 D_c^{-0.13}$. Using such, [2] were able to show that the continuous ejecta blankets on the Moon and Mercury measured by [7] could be close to geometrically similar if compared in terms of transient crater diameter.

Holsapple (1993): Holsapple presented, in his review of crater scaling, a new model for complex crater scaling, also based on volume conserving geometric restoration, but using improved functional forms for the ejecta blankets of craters derived from laboratory experiments in sand [e.g., 4]. Although details were not given, the overall functional form is familiar:

$$D = 1.02 D_c^{-0.086} D_{tr}^{1.086} . \quad (3)$$

A slightly different form was given in terms of transient excavation radius, which presumably refers to the ground plane.

Comparisons: All three scaling laws have similar forms but clearly different exponential dependences. They cannot all be correct. Each scaling law uses a different definition or value for D_c on the Moon, as well, which complicates comparisons. In terms of an "equivalent simple crater," however, eqs. (1-3) predict, e.g., 70.7, 74.1, and 79.7 km, respectively, for the 93-km-diameter Copernicus. We will discuss which of the formulations give too much or too little crater enlargement, and which if any might be considered "just right."

References: [1] Croft S.K. (1985) *JGR, 90, suppl.*, C828–C842. [2] McKinnon W.B. and Schenk P.M. (1985) *LPSC XVI*, 544-545. [3] Holsapple K.A. (1993) *AREPS, 21*, 333–373. [4] Housen K.R. et al. (1983) *JGR, 88*, 2485–2499. [5] Pike R.J. (1977) in *Impact and Explosion Cratering*, Pergamon, 484-509. [6] Grieve R.A.F. and Garvin J.B. (1984) *JGR, 89*, 11,561–11,572. [7] Gault D.E. et al. (1975) *JGR, 80*, 2444–2460.

MODELING METEORITE IMPACTS: WHAT WE KNOW AND WHAT WE WOULD LIKE TO KNOW. H. J. Melosh (Lunar and Planetary Lab, University of Arizona, Tucson AZ 85721. jmelosh@lpl.arizona.edu).

Meteorite impacts can be studied by computer simulation: Large meteorite impacts are among those phenomena that are either too large or too dangerous to study experimentally. Although impacts have affected the formation and surfaces of nearly every body in the solar system, we are limited to observing the results of past events. Investigation of impact processes is thus divided into observational studies of the traces of past impacts, small-scale analogue laboratory experiments and, most recently, detailed computer modeling. Computer models offer the possibility of studying craters at all scales, provided we completely understand the physics of the process and possess enough computer power to simulate the features of interest [1].

But computer models cannot do everything! One of the most common disappointments of geologists not familiar with modeling is that computer simulations cannot answer all questions we might like to ask. Numerical simulations suffer two major shortcomings: One is that they cannot treat processes that are not included in the computer code. Thus, no computer code presently treats the chemical or isotopic interactions that occur during an impact. This does not mean that such processes are untreatable, just that the appropriate codes that embody the correct physics must be created. In some cases the physics is poorly known and research must be done to improve the basic foundations. The second shortcoming stems from resolution in both space and time. All digital computer simulations depend on dissecting time and space into discrete blocks. The number of such blocks is limited by the amount of time and physical memory available for the computation. These limits can be easily exceeded by even an apparently modest computation. Thus, if an investigator wants to know about the dynamics of meter-size ejecta blocks in a 10 km diameter impact crater, he or she may discover that the required resolution far exceeds the capacity of any existing computer (a 3-D computation must include at least 10^12 computational cells!). Models to "predict" the effects of the impacts of Shoemaker/Levy 9 fragments with Jupiter [2] were still running at the time of the impacts, more than a year after the comet was discovered! These limitations can be surmounted both by faster computers with more memory as well as by better solution algorithms, such as the recent adoption of SPH codes when both hydrodynamics and self-gravity are important in a simulation [3].

Before beginning any computer simulation it is important to ask whether the numerical computation is capable of answering the desired question. Are all of the relevant processes included in the code to be used? Can the problem be solved in reasonable time on the available hardware? Too often the answer is "no" and the potential modeler must look elsewhere for enlightenment. But there **are** plenty of open questions that are still ripe for computer solutions.

The three pillars of impact simulation: The physics needed to simulate large meteorite impacts lies squarely in the classical domain. The size scale is so large that quantum effects are not important (although quantum mechanics does determine the thermodynamic equation of state) and the velocities are well below the speed of light, so classical Newtonian mechanics, supplemented by classical thermodynamics, provides an adequate framework for modeling impacts. In addition, it has become clear that successful simulation of real impact craters often requires a detailed understanding of the response of real rocks to stress and heat.

Of these three supporting pillars, Newtonian mechanics is probably the least troublesome. All modern "hydrocodes" (a now obsolete term that reflects the historical development of computer codes that, at first, did not contain material strength) incorporate the standard F = ma foundation of mechanics, although this is often obscured by an impressive amount of bookkeeping to keep track of all the pieces. All codes incorporate some form of gravitational acceleration, although only a few employ self-gravitation (only important in planet- scale impacts). It is notable that there do not appear to be any talks at this conference on this aspect of computer modeling.

The next supporting pillar is thermodynamics, through the equation of state [4]. The equation of state for impact modeling is a little peculiar: Instead of the conventional thermodynamic relation relating pressure P to density ρ and temperature T, $P(\rho,T)$, hydrocodes require a relation between P, ρ and internal energy E. Equations of state for metals have been vigorously pursued by squadrons of physicists since the end of WWII, mainly to support the design and testing of nuclear weapons. However, few good equations of state exist for geologic materials, such as rock or ice. More research is needed to create these important relations.

Finally, in the late stages of an impact event material strength becomes important. Very little work has been done on good strength models for rock [5]. Porosity is also now recognized to play a key role for some impacts, especially on asteroids, which recent research has shown might be as much as 50% porous. Impact crater collapse and the morphology of large craters are controlled by strength, and observations suggest that a poorly understood mechanism must operate to greatly degrade the strength of rocks surrounding an impact site shortly after an impact event

[6].

What next? Our ability to numerically simulate impact events is currently being taxed by a number of difficult problems. We are concerned about the possibility of impacts causing future extinctions, as they did at the K/T boundary. Two and three-dimensional models have already been used to estimate the mass and type of environmentally active gases released by the impact [7], but the ultimate effects of these gases on climate is still largely unknown. Chemical reactions of material in hot vapor plumes may be important for both environmental effects as well as explaining the observed oxidation state and isotopic fractions observed in the ejecta. Several new craters with unusual morphologies such as the Silverpits crater in the North Sea [8] and the Chesapeake Bay crater [9] challenge our understanding of the response of the Earth's surface to large impacts. Crater morphologies on Europa [10] may be indicating the thickness of the ice shell beneath the surface, but we must understand the cratering process better before we can cite a numerical value for the thickness. An active question is whether damaging tsunami result from relatively small impacts in the Earth's ocean. Solving this problem requires a full understanding of interactions near the surface and the physics of wave breaking, a new challenge to existing computer codes.

We currently have a list of urgent needs for making our simulations more realistic. Much work is needed in the near term on equations of state and constitutive models for geologic materials. We will hear more about these needs in subsequent talks. Nevertheless, numerical modeling of impact processes has made important contributions to our understanding of impacts in the past and will surely continue to do so in the future.

References:

[1] Anderson, C.E. (1987) *Int. J. Impact Engineering* **5**, 33.
[2] Zahnle, K. & Mac Low, M.-M. (1994) *Icarus* **108**, 1.
[3] Benz, W. in *Numerical Modeling of Nonlinear Stellar Pulsation: Problems and Prospects* (eds. Buchler, J.R.) 269 (Kluwer Academic, Dortrecht, 1990).
[4] Melosh, H.J. *Impact Cratering: A Geologic Process* 1-245 (Oxford University Press, New York, 1989).
[5] Ivanov, B.A., Deniem, D. & Neukum, G. (1997) *Int. J. Impact Eng.* **20**, 411.
[6] Melosh, H.J. & Ivanov, B.A. (1999) *Ann. Rev. Earth Planet. Sci.* **27**, 385.
[7] Pierazzo, E., Kring, D.A. & Melosh, H.J. (1998) *J. Geophys. Res.* **103**, 28607.
[8] Stewart, S.A. & Allen, P.J. (2002) *Nature* **418**, 520.
[9] Poag, C.W. (1997) *Sed. Geol.* **108**, 45.
[10] Turtle, E.P. & Pierazzo, E. (2001) *Science* **294**, 1326.

SULFUR CHEMISTRY IN K/T-SIZED IMPACT VAPOR CLOUDS. S. Ohno[1], S. Sugita[1], T. Kadono[2], S. Hasegawa[3], G. Igarashi[4], [1]Dept. of Earth and Planetary Science, University of Tokyo (email: oono@space.eps.s.u-tokyo.ac.jp), [2] Institute for Frontier Research on Earth Evolution, Japan Marine Science and Technology Center, [3]The Institute of Space and Astronomical Science, [4]Laboratory for Earthquake Chemistry, University of Tokyo

Introduction: The geologic record indicates that the mass extinction at K/T boundary, 65 Myrs ago, was caused by a hypervelocity impact of an asteroid or a comet [1]. During the K/T impact event, a large amount of sulfur was degassed from the impact site [e.g., 2, 3, 4]. The degassed sulfur converts to sulfuric acid aerosol and stays in the stratosphere for a long time [3, 4]. This reduces the sunlight significantly and leads to a mass extinction. However, if the degassed sulfur is dominated by SO_3 not SO_2, then the conversion to sulfuric acid aerosol occurs very rapidly and the blockage of sunlight does not last for a long time [3, 4, 5]. The chemical reaction of sulfur-oxides in an impact vapor cloud, nevertheless, has not been studied in detail previously, and the SO_2/SO_3 ratio in a vapor cloud is yet highly uncertain. The purpose of this study is to estimate the SO_2/SO_3 ratio in the K/T impact vapor cloud. Here we discuss the results of calculation of chemical equilibrium and kinetics of sulfur-containing species in an impact vapor cloud as well as mass spectroscopic analysis of vapor plumes created by laser irradiation on anhydrite.

Chemical Equilibrium Calculation: We calculated equilibrium chemical composition in vapor clouds generated from calcium sulfate ($CaSO_4$). We assumed several different impact velocities and different types of projectiles for the K/T impact.

The result of the calculation indicates that $SO_2+1/2O_2$ is more stable at high temperatures and high pressures and that SO_3 is more stable at low temperatures and low pressures. Over the entire range of the impact conditions we assumed, the SO_2/SO_3 ratio dramatically changes in the range between 600K and 1000K. If the reaction SO_2+O to SO_3 quenches at a temperature higher than 1000K, most of impact-degassed sulfur is released to the environment as SO_2. However, if the reaction SO_2+O to SO_3 quenches at a temperature lower than 600K, SO_3 is dominant.

Kinetics of Redox Reaction of Sulfur Oxides: We estimate the SO_2/SO_3 ratio in vapor clouds at the quenching temperature using a theoretical evaluation of chemical reaction rate of the reaction SO_2+O+M to SO_3+M [6]. The result of the calculation indicates that the SO_2/SO_3 ratio is smaller for a vapor cloud with a larger mass and that the SO_2/SO_3 ratio in a K/T-size vapor cloud is approximately unity. Because the result of this kinetic model estimation is an upper limit of the SO_2/SO_3, the SO_2/SO_3 ratio in K/T-size impact vapor cloud may have been much smaller than unity.

Laser Irradiation Experiment: A YAG laser beam (1.06μm of wave length, 25-400 mJ of pulse energy, 0.5-2 mm of irradiation spot diameter) was irradiated to a sample of anhydrite in a vacuum chamber. Vapor degassed by laser irradiation was analyzed with a quadrupole mass spectrometer (QMS). The gas sample obtained in every laser irradiation experiment was dominated by SO_2, but SO_3 was also detected. The SO_2/SO_3 ratios measured in experiments were between 80 and 300, and decrease with the laser beam diameter. The dependence of the SO_2/SO_3 ratio on laser beam diameter is $SO_2/SO_3 = 120D^{-0.61}$.

The SO_2/SO_3 ratio in the experiment is about 10^{-3} time that in the kinetic model estimation for the size of vapor clouds produced in the laboratory. Our experimental results also show that the rate of decrease in the SO_2/SO_3 ratio obtained in the laser experiment as a function of vapor mass is higher than that predicted by the kinetic calculation. The power-low relation obtained in the laser experiments predicts that it will be 10^{-6} for a K/T-size impact vapor cloud. This strongly suggests the possibility that SO_3 was dominant in the degassed sulfur by the K/T impact.

Conclusion: Chemical equilibrium calculation indicates that SO_3 is more stable than $SO_2+1/2O_2$ at low temperatures and low pressures. Kinetic model calculation shows that the SO_2/SO_3 ratio in a K/T-size vapor cloud is lass than unity. The SO_2/SO_3 ratio estimated based on the laser-irradiation experiments is about 10^{-6} for a K/T-size vapor cloud. Three lines of evidence strongly suggests that the SO_2/SO_3 ratio in K/T impact vapor cloud may have been much smaller than 1. Then sulfuric acid aerosol may not have blocked the sunlight for a long time. Instead, there may have been an extremely intense global acid rain immediately after (<100 days) the K/T impact.

References: [1] Alvarez, L.W. et al. (1990) *Science, 208,* 1095-1108. [2] Sigurdsson, H. et al. (1992) *EPSL, 109,* 543-559. [3] Pope, K.O. et al. (1994) *EPSL., 128,* 719-725. [4] Pope, K.O. et al. (1997) *JGR, 102,* 21645-1664. [5] Ohno et al, (2002) *Earth Planet. Sci. Lett.,* Submitted. [6] Troe, J., (1978) *Ann. Rev. Phys. Chem., 29,* 223.

IMPACT INDUCED TARGET THERMO-MECHANICAL STATES AND PARTICLE MOTION HISTORIES, John D. O'Keefe,[1] and . Thomas J. Ahrens[1], Lindhurst Laboratory of Experimental Geophysics, California Institute of Technology, Pasadena, CA 91125, dinosr@aol.com

Objectives The first objective of this effort is to determine how the post impact measurable crater features relate to the processes that take place during impact and the second is to the determine from a given suite of measurements the uncertainty in estimating the impactor's parameters.

Approach. We have taken a numerical approach using the CTH code[1] to calculate the evolution of the near field impact process. This includes the details of the early time shock wave driven flow fields, the development and collapse of the transient cavity [2], and in a few limited cases the very late time thermal and stress histories. To quantify the impact process, we placed massless tracer particles in layers that simulate the target stratigraphy (Figs 1-4) and stored the motion and thermo-mechanical state histories (e.g. pressure, temperature, damage, peak stress/strain rate..) of these particles. We took this approach because the late time distributions are significantly different from the initial distributions. We used the ANEOS model for equation of state and a Mohr-Coulomb damage model for the strength degradation by shear strain fracture [2,3]. The key parameters for the impacts are a, the impactor radius, U, the impactor velocity, Yc, target cohesive strength, μ, internal friction, μd, damaged internal friction. We found that we could replicate the key features with values of target material parameters within the magnitudes found in laboratory measurements. We developed scaling laws for the key target metrics based upon the Mohr-Coulomb strength model. This provides a the link between the measureable features and the impactor parameters,. In addition it, bounds the effect of damage on the magnitude of the metrics.

Target Motion Histories and Thermo-mechanicl States..

Shown in Figs 1-4 are the particle motion histories and the melted and damaged (shear fractured) regions for three representative cases: 1) simple crater –strength dominated, 2) transition crater - between strength and gravity regimes, and a 3) basin forming impact represented by the Chixculub event[4].:

The geometry of the flow in the strength dominated case (Fig. 1) is very similar to that of all cases at the time of maximum penetration. The melt has two major zones. The melt layer and melt ejecta. The melt layer is underneath the impact point and is on top the damaged region, The trajectories of the melt particles are shown and labeled at the top of the computational grid.

We found that in the strength dominated region that that the depth of penetration decreases with the magnitude of the internal friction. This is due to the dynamic pressure increasing the local strength.

An example of a transition crater is shown in Fig. 2. In this case the low strength material flows over and covers part of the melt layer.

As an example of the motion histories and thermo-mechanical states in basin forming impacts, we simulated the Chicxulub event. The distribution and extent of the damaged region is critical to the crater flow and determines 1) transient cavity dimensions (e.g. depth of penetration), 2) ejecta lofting angles, 3) occurrence and number of terrace/slump faults and 4) distribution of melt. The radial extent of the damage region that replicates the Chicxulub morphology is ~ 100 km. (Fig. 4). At the time of maximum penetration, the transient cavity geometry is similar to Fig. 1. The transient cavity collapses and compresses the melt layer to a region near the center of the cavity and on top of the damaged material (e.g. Fig.3). After the transient peak collapses, the melt flows in a thin layer over the peak ring (Fig. 4), The peak ring is formed by the collision of the downward flowing transient peak with the nearly vertically launched transient cavity flow. Note that while the transient central peak is moving upward that the ejecta curtain is still impacting the surface and that slumping is occurring in front of the ejecta curtain (Fig. 3). In addition, an asymmetric fault (diameter = 150 km) is formed that bounds the terraced zone and extends downward to the Moho. This feature has been interpreted as the crater rim [4]. On the other hand, the radius of the overturned stratigraphy (Fig 4), which is a measure of the transient cavity size is probally a more accurate determinant of the energy of impact [5]. Further out, a 200 km diameter exterior ring is formed as a result of secondary impact of ejecta on the damaged region. The Mohr-Coulomb scaling accounts for basin forming impacts and shows the effect of internal friction on depth of penetration and quantifies the effect of overburden pressure.

References [1]McGlaun, J and S.L. Thomsen *Int. J. Impact Eng.*(1990)**10**,360-361,.[2] O'Keefe, J.D. and T.J. Ahrens (2001)*Int. J. Impact Eng.*,**36**,17.011-17,038. [3] Johnson, G.R. and T. J. Holmquist. (1994) High Pressure Science and Technology, 981-984 [4] Morgan , J., *et a.l* (1997)Nature, **370**, 472-476, [5] O'Keefe, J.D. and T.J. Ahrens (1999) *JGR* ,**10(E11)**27,091-27,1093

PARTICLE MOTION HISTORIES: J. D. O'Keefe and T.J. Ahrens

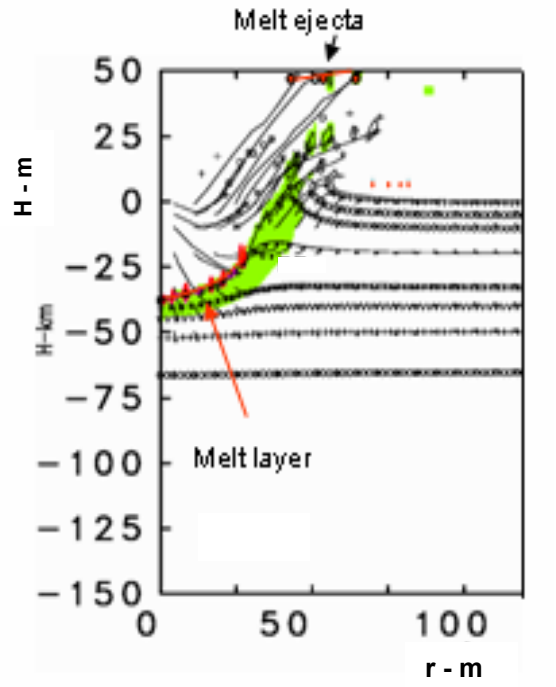

Fig. 1. **Strength dominated crater**. Particle motion histories and melted and fractured regions. Time = 0.15 s U=20 km/s, a = 5 m, Yc = 1.0e9, μ = 0.75, μd = 0.1, εf = 0.05., g = 0.0 m/s^2. Damage colors shown in Fig.3

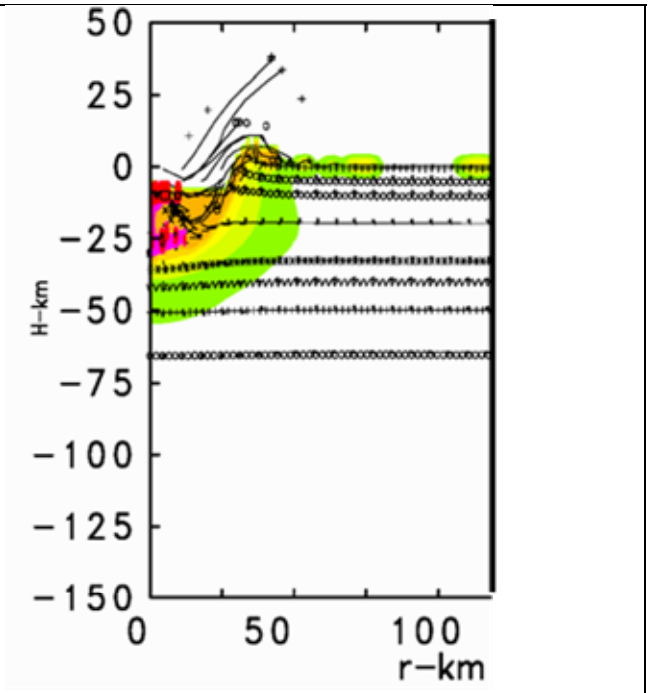

Fig. 2 **Transition crater**. Particle motion histories and - melted and fractured regions. Time = 39 s,. U=20 km/s, a = 5 km, Yc = 0.0, μ = 0.75, μd = 0.1, εf = 0.05, g = 9.8 m/s^2. Damage colors shown in Fig.3

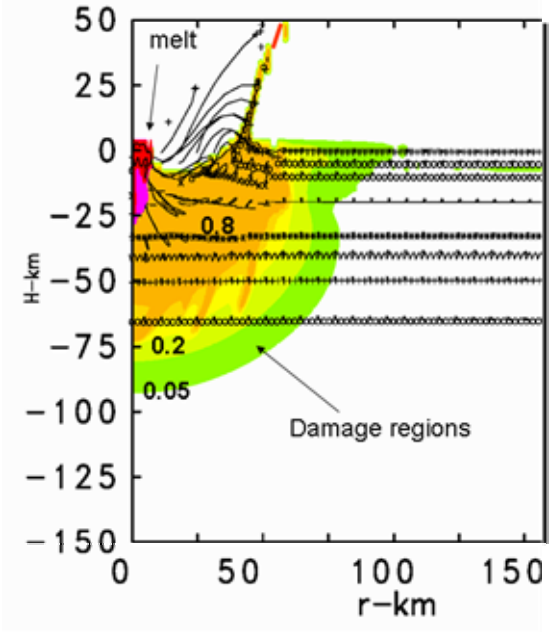

Fig. 3 Complex crater. Chicxulub. Time = 88 s.. U=20 km/s, a = 5.0 km, Yc = 2.4e9, μ = 0.75, μd = 0.1, εf = 0.05. g = 9.8 m/s^2. Note dips in damage region indicating faulting.

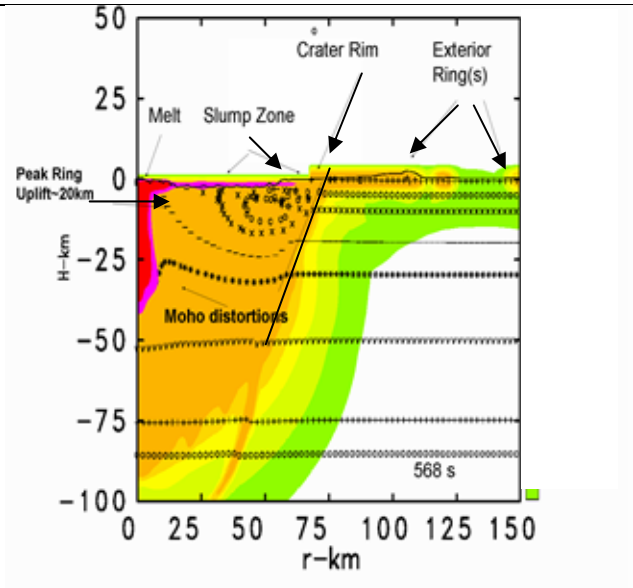

Fig. 4 3 Complex crater. Chicxulub. Time = 568 s. U=20 km/s, a =7. 5 km, Yc = 1.0e9, μ = 0.75, μd = 0.2, εf = 0.1, g = 9.8 m/s^2.Note dips in damage region indicating faulting. Damage colors shown in Fig.3.

Velocity Distributions of Fragments and its Time Dependence

N. Onose and A. Fujiwara, The Institute of Space and Astronautical Science, 3-1-1 Yoshinodai, Sagamihara, Kana-gawa, 229-8510, JAPAN, onose@planeta.sci.isas.ac.jp

Introduction: Oblique impact cratering experiments were done, and the fragment size and velocity were measured for fragments larger than 1mm in diameter, and slower than 200m/sec. A high speed CCD video camera was used to see the fragments in flight, and secondary collisions with a window of the target chamber. The purpose of this paper is to provide a database of fragments velocity, which is essential to deeper understanding of the surface evolution of small aster-oids.

Experimental Procedure: A two-stage light-gas gun was employed, and impact velocities are around 4km/sec. A high-speed CCD video camera of 4500frames/sec and 9000frames/sec enabled us to track fragments in flight, and to measure the locations and the times of the secondary collisions. A target box with a slit of15mm width was employed to limit the ejection in the plane including the trajectory of the projectile.

Results: An example of the time dependence of the ejection pattern is shown in figure 1. In this run a target box with a slit was employed. Ejection is divided into 4 stages according to the ejection pattern. The first stage (order of μsec) corresponds to ejection of very fine and fast fragments like jetting and the earliest conical ejecta cloud, and these particles could not be traced individually. Their typical size is less than 1mm in diameter, and velocity is over 1km/sec. The ejecta in the second stage (0-3msec) consists of 0.1 to 1mm fragments ejected conically at a few hundreds m/s, and at an ejection angle higher than about 60degree from the target surface. The 3D velocity derived from the secondary collisions also shows that the ejection at the second stage is conical. In the third stage (1-10msec), larger spall fragments, about 1cm in diameter, ejected in a cone narrower than that of the second stages. And a cluster of small and slow fragments (0.1-5mm in diameter and a few m/sec) ejected nearly perpendicular to the target surface characterizes the last stage (3msec-). 3/4 fragments are ejected normal to the target surface slower than 6m/s at this stage.

To discuss the size-velocity correlations, three results from the experiments of 7mm nylon sphere on gypsum target at about 4km/sec at 0degree, are shown in Fig. 2. The line in Fig. 2 shows the mass-velocity relation fit for the fragments ejected earlier than 5msec. The velocity of Fragments in this stage can be expressed as follows.

$$v_{spall} = 6 \times m_{spall}^{-0.16}$$

It should also be noted that up to 90% of perticles in number is slow (0.1 - 10m/sec), and small (less than 2mg) fragments.

Acknowledgements: We must thank Dr.s Mizutani, and Kato for their useful suggestions.

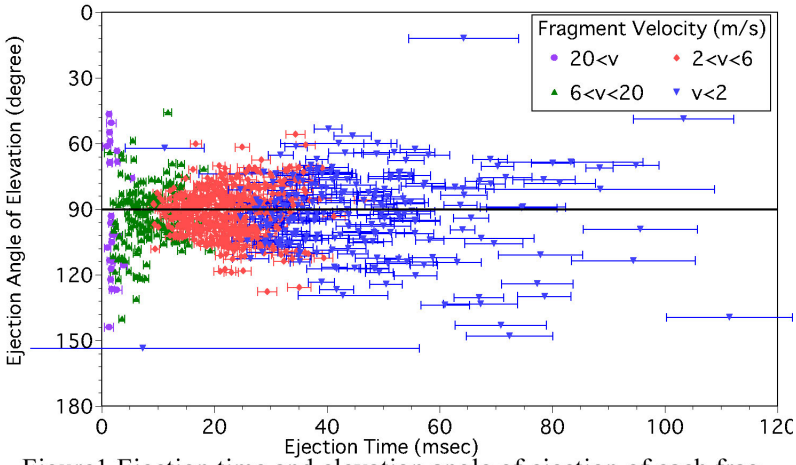

Figure1 Ejection time and elevation angle of ejection of each fragment in the impact at 0degree.

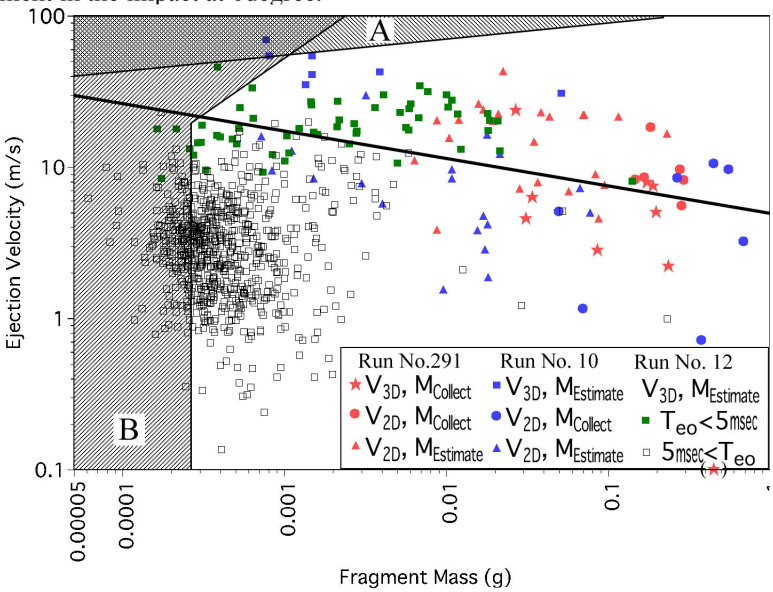

Figure 2 Fragment radius and ejection velocity of 0degree Impact: Area A and B represent the region which is difficult to measure because of too fast and too small, respectively.

Velocity Distributions of Fragments in Oblique Impact Cratering on Gypsum

N. Onose and A. Fujiwara, The Institute of Space and Astronautical Science, 3-1-1 Yoshinodai, Sagamihara, Kanagawa, 229-8510, JAPAN, onose@planeta.sci.isas.ac.jp

Introduction: In order to understand the behavior of the impact-induced fragments on the small asteroid, oblique impact cratering experiments were produced using gypsum targets, which were used as one of porous and low density materials. The fragment size and velocity were measured for fragments larger than 1mm in diameter, and slower than 200m/sec. A high speed CCD video camera was used to see the frag-ments in flight, and secondary collisions with a win-dow of the target chamber were also employed to measure fragment velocity. Especially, we focused to measure the behaviors of very low velocity fragments, which have special meaning for the ejecta on very small asteroids.

Experimental Procedure: We used almost the same experimental procedure as our other paper pre-sented in this meeting, Velocity Distributions of Frag-ments and its Time Dependence. Since in this series of oblique impact, we shot the target surface inclined downward, the extremely slow fragments could come out from the crater cavity.

Results: In the paper cited above, it is shown that the impact ejection is divided into 4 stages according to the ejection pattern. In the second stage (0-3msec), the elevation angle of ejection decreases slightly, and the data are more scattered compared with the case of verti-cal impact, in the impact at 45degree. In the impact at 70 degree, the secondary collision on the window only was identified in the down range direction, and that was also consistent with the result of the run using witness papers.

Figure 1 indicates the ejected time and the elevation angle of ejection of the each tracked fragments also mentioned in the other paper for the vertical impact one. In the impact at 0degree, and 45degree, a target box with a slit was installed to get the 3D velocity of the fragments, and there is few fragments were ejected target surface normal in the second stage. The large number of small and slow fragments ejected later, consists the last stage (3msec-). The average direction of the flow composed by a cluster of small and slow fragments slightly deviate from the surface normal in the oblique impact.

Acknowledgements: We must thank Prof. Mizu-tani, Prof. Kato, and persons in ISAS who gave us important suggestions.

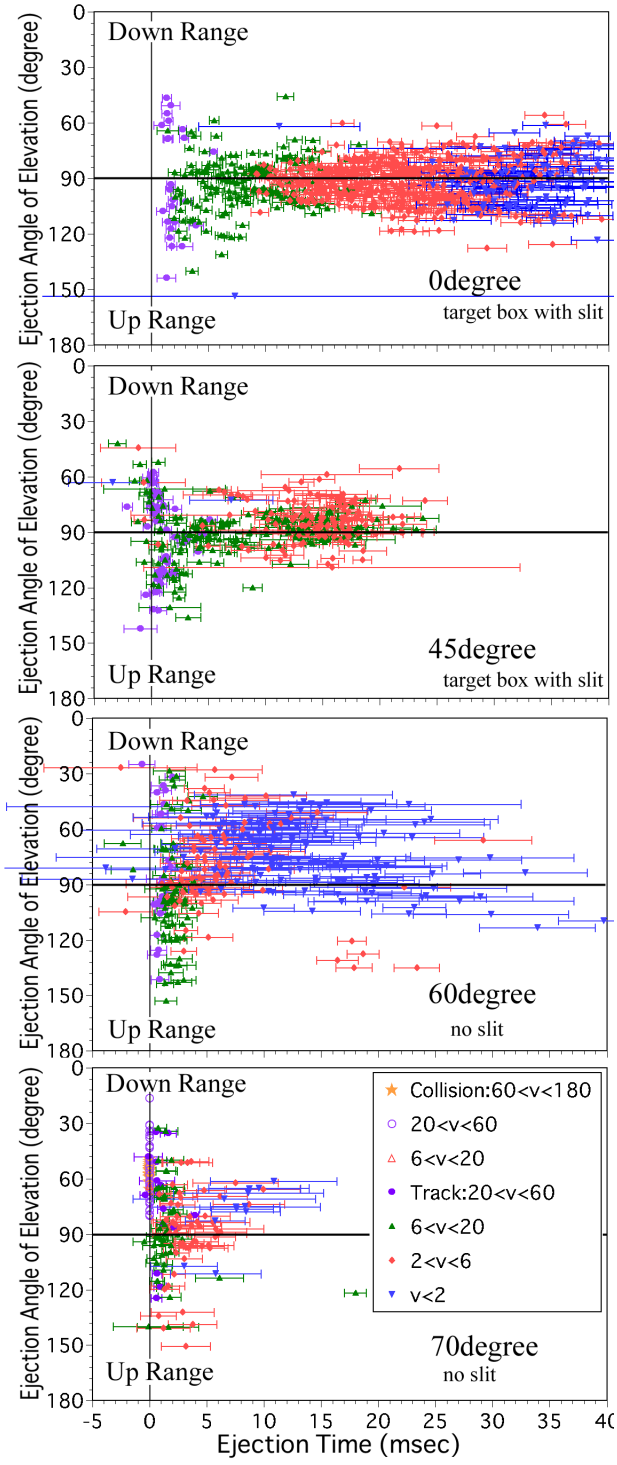

Figure 1 Ejected time and the elevation angle of ejection in the oblique impacts: the later half of the film in the impact at 70degree was lost by an accident.

NEXT STEP IN MARINE IMPACT STUDIES: COMBINING GEOLOGICAL DATA WITH NUMERICAL SIMULATIONS FOR APPLICATIONS IN PLANETARY RESEARCH. J.Ormö[1] [1]Centro de Astrobiologia (CAB), Instituto Nacional de Técnica Aeroespacial, Ctra de Torrejón a Ajalvir, km 4, 28850 Torrejón de Ardoz, Madrid, Spain. (ormo@inta.es)

Introduction: Baltoscandia is favourable for geological studies of marine-target (M-T) craters. One reason is the relatively dense population of craters of different diameters, of approximately the same age, and with different target water depths. This allows comparative studies of the effects of a target water layer on the lithologies and morphologies of the resulting craters [1]. Baltoscandian craters like Kärdla [2] and Lockne [3] are well documented. Today, a considerable number of the documented craters and impact sites on Earth are known to have formed at sea. All but one, the Eltanin impact site west of Chile, have formed in epicontinental seas. This circumstance is mainly a result of higher probability of both formation and preservation in such areas [1]. Famous craters as Chicxulub, Chesapeake Bay, and Mjölnir were also formed at sea [e.g. 4, 5, 6]. Marine impact cratering is an important topic within impact research. The fact that our planet is mostly covered by water must be taken into consideration when evaluating consequences and hazards from impact events. In addition, M-T craters may have applications in the exploration of our Solar System.

Definition: An M-T crater forms from an impact into a target with an upper layer of water. In its transient stage, an M-T crater consists of a water cavity and, in some cases, a seafloor crater. Only the latter may be preserved. How much of the crater that develops in the seafloor depends on the amount of expended energy in relation to the depth of the sea. This relation has been analysed both experimentally [7] and numerically [8]. Studies by Ormö and Lindström [1] show a strong link between the water depth and the geology of the seafloor crater. At relatively shallow water depth the crater resembles a "land-target" crater, although sometimes with stronger collapse of the rim. At deeper water the crater is concentric with a deep crater in the basement surrounded by an outer crater, apparently formed by a shallow excavation flow in connection with the development of a wide water cavity [1, 8, 9]. The outer crater may in these cases be cut by gullies eroded by the resurge of debris-loaded water.

The potential of numerical simulation: Geological studies of the Lockne crater have improved our understanding of water related features to such an extent that they can be used as constrains not only for a rough simulation of the impact, but for modeling specific parameters. The codes have likewise developed so that they now better can simulate the complex process of an impact into a layered target. This development led to an attempt to make a detailed numerical modeling of the 455 Ma Lockne crater [9]. The aim was primarily to find the target water depth, which was an unknown variable, but also to better understand the processes behind some of the special features of the crater (e.g. the development of a wide overturned flap). The model also gave the opportunity to test the code on a full-scale impact in a layered target. Main geological constraints in the Lockne modeling were (1) the occurrence of a 7.5 km wide inner crater in the crystalline basement with a slightly elevated rim, (2) a shallow outer crater with no obvious rim, (3) an about 3 km wide, overturned flap of basement rock outside the basement crater rim, (4) strong stripping of an initially 80 m thick sedimentary cover prior to the deposition of the flap, and (5) evidence for a forceful resurge. The simulations were done at various water depths of the likely depth interval (200-1000 m). Impactor size, mass, and velocity were also varied. It was concluded that for a 400 m radius asteroid striking at 20 km/s, the target water depth was slightly less than 1000 m. The study is continued with more sophisticated software (3D) to analyse the effects of impact angle and ejecta/water interactions [10].

Perspectives: Knowledge of M-T craters can be used when analysing planetary paleoenvironments and surface properties where remote sensing may provide the only information. Ormö and Muinonen [11] propose that Martian M-T craters could reveal paleo-water depths and, hence, the climatic evolution of the planet. Any low-strength material in the upper part of a layered target may respond as a water layer. Craters from impacts into hydrocarbon and nitrogen seas have indeed been suggested to exist on Titan [12]. Cassini radar data may reveal their features. Future studies of M-T craters should focus on the mechanics of the concentricity, and the influence of obliquity on the ejecta distribution, resurge flow, and how they affect tsunami formation. This is currently pursued by the new impact research group at CAB by combining experiments, fieldwork, planetary research, and numerical modeling.

References: [1] Ormö J. and Lindström M. (2000) *Geol.Mag*, 137, 67-80. [2] Puura V. and Suuroja K. (1992) *Tectonophysics*, 216, 143-156. [3] Sturkell E. (1998) *Geol. Rundsch.*, 87, 253-267. [4] Morgan J. et al. (1997) *Nature*, 398, 472-476. [5] Poag C.W. (1997) *Sed. Geol.*, 108, 45-90. [6] Gudlaugsson S.T. (1993) *Geology*, 21, 291-294. [7] Gault D.E. and Sonett C.P. (1982) *Geol. Soc. Am. Spec. Paper*, 190, 69-92. [8] Shuvalov V.V. and Artemieva N.A. (2001) *LPS XXXII*, Abstract #1122. [9] Ormö, J. et al. (2002) *JGR-Planets*, in press. [10] Shuvalov V.V. et al. (2002) *Advances in Impact Studies*, submitted. [11] Ormö J. and Muinonen P. (2000) *LPS XXI*, Abstract #1266. [12] Lorenz R.D. (1997) *Planet. Space Sci.*, 45, 1009-1019.

COMPLEX CRATER FORMATION AND COLLAPSE: OBSERVATIONS AT THE HAUGHTON IMPACT STRUCTURE, ARCTIC CANADA. G. R. Osinski, J. G. Spray, Planetary and Space Science Centre, University of New Brunswick, 2 Bailey Drive, Fredericton, NB E3B 5A3, Canada. (osinski@lycos.com).

Introduction: It is generally believed that the processes involved in the formation of an initial transient crater and its subsequent excavation, are common for all craters, regardless of their size. A critical assumption is that the depth/diameter ratio of a transient crater remains constant for any given crater size [1,2]. The morphological diversity of impact structures is, therefore, attributed to the modification or collapse of an initial simple hemispherical transient crater [e.g., 2]. The mechanisms of impact crater collapse remain one of the least understood stages in the impact cratering process. Indeed, standard strength models used in conventional hydrocode modeling techniques are not successful in describing crater collapse [2]. Numerical models have also rarely been constrained by field data from terrestrial impact structures. This is, however, a catch-22 situation because very few detailed field investigations of the tectonics of complex impact structures have been made.

Here, we present new constraints on the formation of complex impact craters based on detailed field studies of the Haughton impact structure, Arctic Canada.

Geological setting: The 23 Ma, 24 km diameter Haughton impact structure has been the focus of detailed field investigations over the course of 4 field seasons (1999-2002) as part of the PhD thesis of GRO. Haughton is superbly exposed due to the prevailing polar desert environment. The target rocks consist of 1880 m of almost flat lying sedimentary rocks overlying Precambrian metamorphic basement. Key stratigraphic horizons provide evidence for the depth of excavation and amount of structural uplift and deformation.

Reconstruction of the transient crater: Questions remain as to the exact size of the transient crater at Haughton. Seismic reflection data suggest a diameter of ~12 km [3]. The presence of basement gneisses in the crater-fill melt rocks indicates a depth of excavation (H_{exc}) between 1880 m and ~2200 m. It is generally considered that the depth of the transient crater (H_{tc}) is ~2-3 times greater than H_{exc} [4]. This would yield a H_{tc} of ~4-6 km for Haughton. However, this is incompatible with our field studies and previous seismic investigations [3] that do not indicate significant deformation and displacement of the Precambrian basement (depth to upper surface: 1880 m).

Modification of the transient crater: Our work has revealed that the tectonic modification of the early-formed Haughton crater involved the complex interaction of a series of interconnected concentric and radial faults.

Radial faults. Radial faults record predominantly oblique strike-slip movements. There is generally little (<10 m) or no displacement of marker beds across radial faults. This is despite the fact that substantial volumes of fault breccia (>8 m) are typically present. Importantly, these radially orientated faults are cut and offset by later concentric faults.

Concentric faults. It is noticeable that the intensity and style of concentric faulting changes around the periphery of the crater. They are predominantly listric extensional faults with rotation of beds in the hanging-wall up to ~75°. The outermost concentric faults generally dip in towards the centre of the crater. We suggest that these faults were initiated during the inward collapse of the crater walls. The innermost faults, however, tend to dip away from the crater centre and may represent the outward collapse of the central uplift. The outermost concentric faults typically display two episodes of deformation: (1) early major dip-slip extensional movement; (2) later minor oblique strike-slip movement resulting in the offset of radial faults. A zone of (sub-) vertical faults and bedding occurs along the edge of the central uplift (~6 km radius). This suggests complex interactions between the outward collapsing central uplift material and the inward collapsing crater walls.

Comparison with models: It appears that the transient crater at Haughton was significantly shallower than current models for the cratering process predict. This may suggest a decrease in the depth/diameter ratio of transient craters with increasing crater size. This will have important implications for estimating the size of deeply eroded large impact craters (e.g., Vredefort).

Field studies at Haughton indicate that deformation during the modification stage of complex impact crater formation was brittle and localized along discrete fault planes. We find no evidence to support the hypothesis of 'acoustic fluidization' throughout the whole crater. The presence of little offset along radial faults, despite the large thicknesses of fault breccia, may suggest limited block oscillation along discrete fault surfaces as proposed by Ivanov et al. [5]. However, the scale seen in the field at Haughton is greater than in the models [5].

Acknowledgments: This work represents part of the PhD thesis of GRO and was funded by the Natural Sciences and Engineering Research Council of Canada (NSERC) through research grants to JGS.

References: [1] Grieve R. A. F. et al. (1981) *LPS XII*, 37-57. [2] Melosh H. J. and Ivanov B. A. (1999) *Annu. Rev. Earth Planet. Sci., 27,* 385-415. [3] Scott D. and Hajnal Z. (1988) *Meteoritics & Planet. Sci., 23,* 239-247. [4] Melosh H. J. (1989) Impact Cratering: A geologic process. Oxford University Press, 245 pp. [5] Ivanov, B. A. et al. (1996) *LPS XXVII*, 589-590.

IMPACT MELTING IN SEDIMENTARY TARGET ROCKS? G. R. Osinski[1], J. G. Spray [1] and R. A. F. Grieve[2], [1]Planetary and Space Science Centre, University of New Brunswick, 2 Bailey Drive, Fredericton, NB E3B 5A3, Canada. [2]Earth Sciences Sector, Natural Resources Canada, Ottawa, ON K1A OE8, Canada (osinski@lycos.com).

Introduction: Sedimentary rocks are present in the target sequence of ~70% of the world's known impact structures [1]. One of the outstanding questions in impact cratering studies is: do sedimentary rocks undergo impact melting? This question cannot be addressed through experimentation in the laboratory, which is limited to impact velocities generally below that required for wholesale melting [2]. Numerical and computer-based modeling may offer some important information, however, as Pierazzo et al. [3] note, "there is no good model for melt production from impact craters in sedimentary targets". Studies of naturally shocked rocks, therefore, offer the only true ground-truth data on the response of sedimentary rocks to impact. We have carried out detailed field and analytical studies of naturally shocked sedimentary rocks that will hopefully provide constraints for future modeling.

Physics of impact melt generation: Theoretical considerations of the impact process reveal some important results regarding the generation of impact melt [4]: (i) the volume of target material shocked to pressures sufficient for melting *are not* significantly different in sedimentary or crystalline rocks; (ii) Hugoniot curves indicate that *more* melt should be produced upon impact into sedimentary targets as compared to crystalline targets. Impacts into sedimentary targets should, therefore, produce as much, or even greater volumes of, melt as do impacts into crystalline targets [4].

Where have all the melts gone? It is generally considered that the high volatile content of sedimentary rocks results in the "unusually wide dispersion" of impact melt [4]. However, it is becoming increasingly clear that such lithologies can undergo shock-melting and are preserved in significant quantities in some impact craters.

Haughton impact structure: The target rocks at the 24 km diameter, 23 Ma Haughton structure comprised a ~1750 m thick series of sedimentary rocks (predominantly carbonates, with minor evaporites, sandstones and shales), overlying Precambrian metamorphic basement. Osinski and Spray [5] have recently interpreted the crater-fill deposits at the Haughton impact structure as carbonatitic impact melt rocks. Importantly, the volume of these crater-fill deposits (>12 km^3) is roughly equal to the observed impact melt volumes for comparably sized craters developed in crystalline targets (e.g., >11 km^3 melt at Bolytsh (diameter 24 km) [6]).

Ries impact structure: The 24 km diameter, 15 Ma Ries impact structure comprised a target sequence of ~ 850 m sedimentary rocks (limestone in upper parts, predominantly sandstones in lower parts), overlying Hercynian granites and gneisses. Carbonate melts have been documented at the Ries impact structure by Graup [7] and Osinski [8]. In addition, Osinski [8] has also recognized the presence of SiO_2-rich impact glasses that were clearly derived from sandstones in the lowermost part of the sedimentary sequence.

Implications: Based on our studies of the Haughton and Ries structures, we suggest that sedimentary rocks can undergo shock-melting during impact events. Thus, it should NOT be assumed that all sedimentary rocks and minerals completely degas and disperse at pressures sufficient for melting. This will have implications for the way in which we model the cratering process.

Modeling: The Ries impact event has recently been the focus of numerical modeling studies and 3D hydrocode simulations [9]. These models suggest substantial melt generation from sandstones in the sedimentary sequence, seemingly at odds to the general held view that these lithologies were not shock-melted [e.g., 10]. Recent studies by Osinski [8] have shown that sandstone-derived melts are present. This is an instance where modeling and field studies clearly agree. This is not the case when carbonates are considered. All models to date have considered that carbonates are completely degassed above a certain pressure threshold (e.g., >55 GPa in [9]). This is despite the fact that carbonate melts are known to occur in the Ries and other structures. We suggest that the melting of carbonates should be included in any future modeling studies.

Acknowledgments: This work represents part of the PhD thesis of GRO and was funded by NSERC through research grants to JGS. Financial support for fieldwork at the Ries impact structure came from the Eugene Shoemaker Impact Cratering Award presented to GRO.

References: [1] Earth impact database (2002) http://www.unb.ca/passc/ImpactDatabase/index.htm. [2] Grieve R. A. F. and Cintala, M. J. (1992) *Meteoritics & Planet. Sci., 27*, 526-538. [3] Pierazzo et al. (1997) *Icarus, 127*, 408-423. [4] Kieffer, S. W. and Simonds, C. H. (1980) *Rev. Geophys. Space Phys., 18*, 143-181. [5] Osinski G. R. and Spray J. G. (2001) *EPSL, 194*, 17-29. [6] Gurov, E. P. and Gurova, E. P. (1985) *LPSC XXII*, 310-311. [7] Graup G. (1999) *Meteoritics & Planet. Sci., 34*, 425-438. [8] Osinski, G. R. (2002) *Meteoritics & Planet. Sci.,* (in review). [9] Stöffler et al. (2002) *Meteoritics & Planet. Sci.*, (in press). [10] Englehardt et al. (1995) *Meteoritics & Planet. Sci., 30*, 279-293.